CHEMISTRY
A European Journal

A Journal of
ChemPubSoc Europe

Accepted Article

Title: Polar organofluorine substituents: Multivicinal fluorines on alkyl chains and alicyclic rings

Authors: David O'Hagan

To be cited as: *Chem. Eur. J.* 10.1002/chem.202000178

Link to VoR: http://dx.doi.org/10.1002/chem.202000178

Supported by
ACES

WILEY-VCH

10.1002/chem.202000178

Polar organofluorine substituents: Multivicinal fluorines on alkyl chains and alicyclic rings

David O'Hagan

School of Chemistry, University of St Andrews, North Haugh, St Andrews, KY16 9ST, UK.

E. mail: *do1@st-andrews.ac.uk*

Abstract: This *Review* outlines the progression, primarily of our own work, but with important contributions from other labs, on the synthesis and properties of multiple vicinally fluorinated alkyl chains and rings. Chain conformations of individual diastereoisomers with –CHF- at adjacent carbons are influenced by stereoelectronic factors associated with the polar C-F bond and the polarised geminal hydrogens. Generally the chain will prefer a conformation which acts to minimise overall molecular polarity, and where the C-F bonds orient away from each other. However when vicinal fluorines are positioned on a ring then conformations are more constrained. The ring will adopt optimal conformations such as a chair in cyclohexane and then C-F bonds can be introduced with a stereochemistry that forces parallel (axial) orientations. In the case of cyclohexane, 1,3-diaxial arrangements of C-F bonds impart considerable polarity to the ring, resulting in an electronegative 'fluorine face' and an electropositive 'hydrogen face'. For all-*syn* 1,2,3,4,5,6-hexafluorocyclohexane, this arrangement generates an unusually polar aliphatic ring system. Most recently the concept has been extended to the preparation of all-*syn* 1,2,3-trifluorocyclopropanes, a rigid ring system with fluorines on one face and hydrogens on the other. Log Ps of such compounds indicate that they are significantly more polar than their parent alicyclic hydrocarbons and give some positive indication for a future role of such substituents in medicinal chemistry. Expanding to such a role will require access to improved synthesis methods to these motifs and consequently access to a broader a range of building blocks, however some exciting new methods have emerged recently and these are briefly reviewed.

Introduction

Selective fluorination has emerged as an important tool in modern medicinal chemistry.[1] There are particular properties of fluorine which make it attractive in this regard.[2, 3] It forms stable mono-covalent bonds to carbon. It is sterically compact, and it has a limited propensity to make intermolecular contacts. In these respects fluorine has some similarities to hydrogen. However

10.1002/chem.202000178

there are consequences too, to introducing fluorine due its high electronegativity.[2,3,4] It differs from hydrogen in that such a replacement can alter lipophilicity, or it can offer adventitious benefits most typically protecting against the oxidative metabolism of bio-actives.

Intramolecular inductive effects from this most electronegative atom influence the acidity/basicity of neighbouring functional groups and the polarised C-F bond generates localised dipoles which can influence molecular conformation, effects not associated with hydrogen. Fluorine is commonly discussed[5] for its capacity to increase lipophilicity (Log P) when an aryl-H to aryl-F substitution is made, a situation that becomes much more significant with aryl-CF_3[6] or aryl-OCF_3.[7] Generally increasing lipophilicity is not a desirable direction of travel in drug discovery programmes, however a feature of fluorine that is less widely appreciated is that selective fluorination of aliphatics, rather than aromatics, tends to decrease lipophilicity. Műller and colleagues[8] have most convincingly articulated this, demonstrating that Log Ps tend to decrease with selective fluorinations and an aspect of this is briefly summarised in Figure 1(a) where aryl fluorinations increase, but partial alkyl fluorinations decrease Log P.

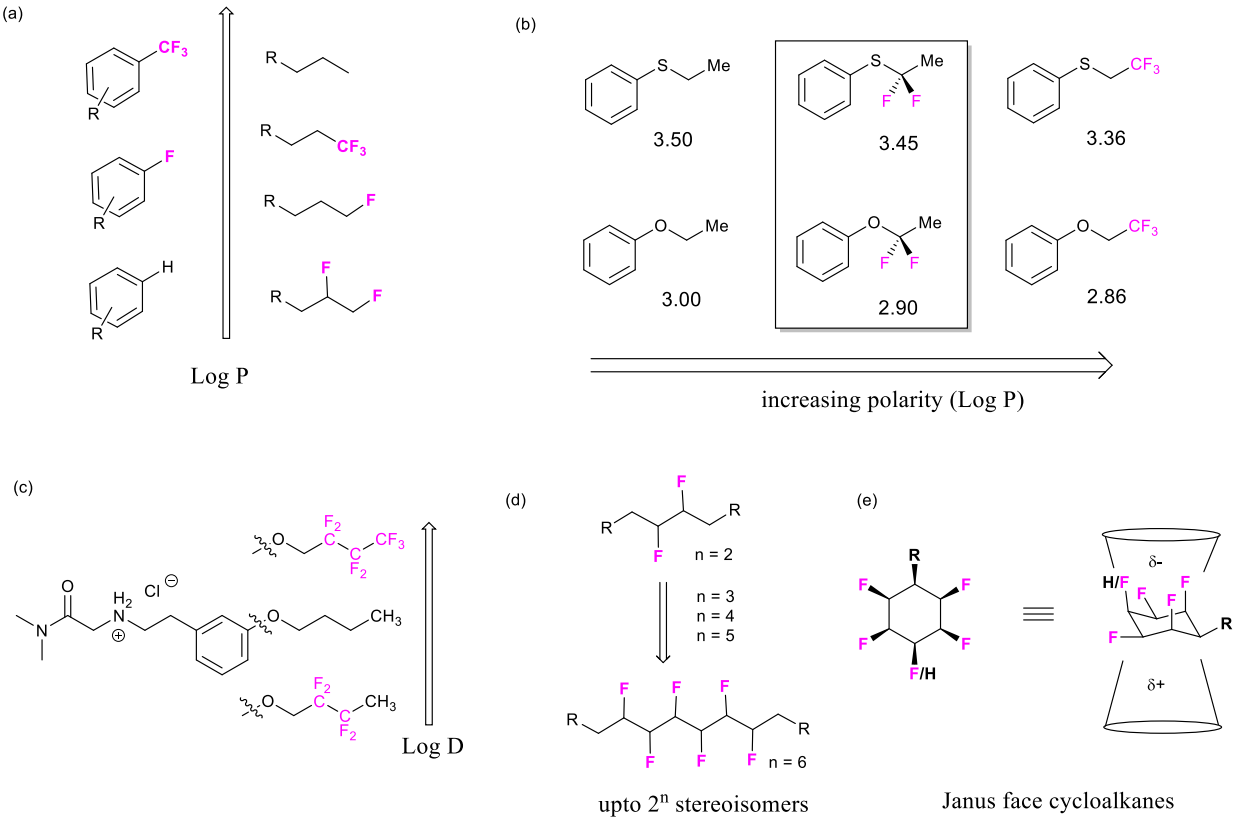

10.1002/chem.202000178

Figure 1 Partially fluorinated motifs: (a) Opposite polarity trends between aryl and alkyl fluorination; (b) Partially fluorination of ethers lowers Log P; (c) Partial perfluoro-chains become polar; (d) Mutivicinal fluoroalkanes; (e) 'Janus face' all-*syn* fluoro cycloalkanes.

Typical locations for fluorine (aryl-F, CF_3 groups) are represented in the new fluorine containing drugs **1** – **10** that were licenced by the FDA in 2019[9]. The structures are shown in Figure 2. Most appear to incorporate fluorine to increase lipophilicity and/or block metabolism, however upadacitinib **6** and ubrogepant **10** have CF_2CH_2N-motifs which can be expected to increase polarity certainly relative to their EtN- analogues as the CF_3 will polarise the vicinal hydrogens and in the case of ubrogepant **10**, increase the acidity (H-bond acceptor ability) of the proximal NH.

10.1002/chem.202000178

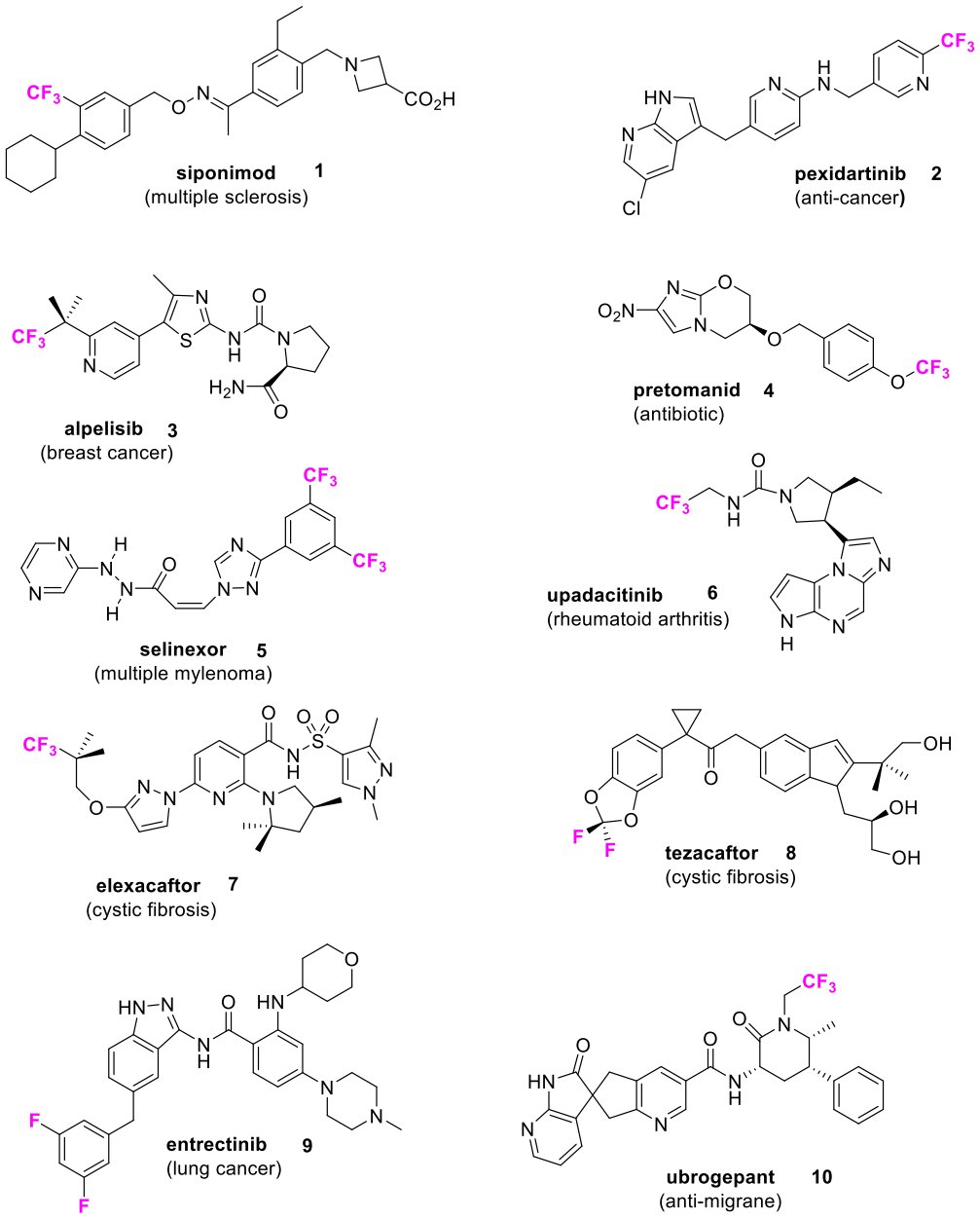

Figure 2. Fluorine containing drugs **1 - 10** approved by the FDA in 2019.[9]

We,[10] and others,[2,11] have been interested in exploring the properties of mixed fluorocarbon/hydrocarbon alkyl motifs such as Ar-CF_2H, Ar-O-CF_2H, Ar-O-CF_2CH_3 and Ar-S-CF_2CH_3. These are more polar than the parent alkyl aliphatics as illustrated in Figure 1 (b), and even for perfluoroalkyl chains, Linclau[12] has recently shown that replacement of the terminal fluorines going from RCF_2CF_3 to RCF_2CH_3 significantly increases polarity (decreases Log D) (Figure 1 (c)). Our interest[13] in this area has extended to preparing alkyl chains[14-17] and

alicyclic rings[18-20] (Figures 1 (d) and (e) respectively) with multiple vicinal fluorines, compounds which can become suprisingly polarity, particularly in ring systems.

Sequentially fluorinated alkyls, have an increasing number of stereoisomers as the length of the chains increase, and therefore synthesis approaches have to be designed to navigate this stereochemical complexity. Our programme has progressed from linear alkyl chains containing two to six vicinal fluorines,[14-17] and then we have addressed cycloalkanes[18-20] of this class as illustrated in Figure 1(c & d). For the rings, specific isomers were targeted such that the fluorines occupy one face only of the alicyclic rings, and with the hydrogens of the fluoromethylene groups, occupying the other face. We find that this stereochemical arrangement maximises the polarity of the ring as illustrated in Figure 1(d) and these have been termed[21] 'Janus face' ring systems due to the electronegative (fluorine) and electropositive (hydrogen) faces.

Vicinal difluorides

This programme had its origins in the fluorine '*gauche* effect',[22] although in the end this emerged to offer a rather weak conformational bias and is not a dominating influence. The fluorine '*gauche* effect' is a descriptor which recognises that 1,2-difluoroethane **11** is lower in energy (~0.8 – 1.0 kcal mol^{-1}) when the two fluorines orient *gauche* with respect to each other, rather than *anti*. The *anti*-conformation would perhaps be anticipated to be lower in energy based on sterics and electronic repulsion between the fluorines, and indeed this is the dominant isomer in the case of 1,2- dichloro-, dibromo- and diiodo- ethanes, however stereoelectronic effects favour a *gauche* conformation for 1,2-difluoroethane. The most obvious explanation is that the electrons in the C-H sigma bonding orbital (σ_{CH}) align antiperiplanar to the C-F antibonding orbital (σ^*_{CF}), and derive stabilisation by hyperconjugation (HOMO σ_{CH} to LUMO σ^*_{CF}) between these two orbitals. This analysis is borne out by theory studies and particularly those exploring Natural Bond Orbital (NBO) interactions. Linclau[23] has recently rationalised the non-optimal geometries which are consistently recorded for the lowest energy *gauche* conformer of 1,2-difluoroethane **11** where the *gauche* F-C-C-F angle (72°) is wider and the F-C-C-H *anti-periplanar* angle (170°) narrower than anticipated.

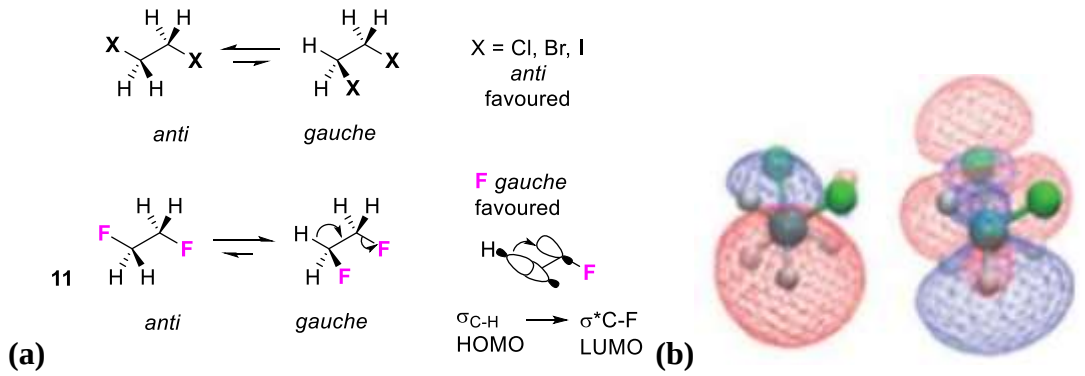

Figure 3. (a) The fluorine *gauche* effect in 1,2-difluoroethane **11**. (b) The narrowing of the F-C-C-F angle is attributed to better overlap of a skewed (blue lobe) C-H σ- orbital with the σ*C-F (LUMO). Image from reference-23.

They observed that maximal NBO interactions did indeed occur at these apparently non optimal geometries. However the geometry is consistent with maximising the overlap between a skewed C-H σ orbital (HOMO) and a normal σ*C-F orbital (LUMO) as illustrated in Figure 3b. The upper (blue) lobe of the C-H σ (HOMO) orbital is skewed (repelled) by the presence of the geminal fluorine, and a small rotation is required to maximise overlap with the σ*C-F (LUMO) associated with the other C-F bond. The consequence is that the F-C-C-F angle widens and the F-C-C-H angle narrows relative to optimal geometries.

Our first study in this area explored the chain conformations of the *erythro* and *threo* isomers of 9,10-difluorostearic acids **12a** and **12b**. Melting points are very different for these fatty acids, with the *threo* isomer having a significantly higher melting point (88 ºC versus 69 ºC) than the *erythro* isomer. This is consistent too comparing melting point data of other long chain alkyls with *erythro* and *threo* vicinal difluorides such as **13a**/**13b**[24] and **14a/14b**[25] at a central location. In the case of **12a** and **12b** pressure/area Langmuir isotherms of these steric acids were recorded on water and showed clearly that the *threo* fatty acid formed the more stable monolayers. In an extended *zig-zag* conformation, the fluorines are *gauche* to each other in the *threo* isomer and *anti-periplanar* for the *erythro* isomer, consistent with the stabilities observed. However, as appealing as the *gauche* rationale is in this case in terms or arguing stabilities, it does not seem to be the significant underlying factor in determining the differences in properties of these isomer classes. It has been convincing argued by Linclau that the *gauche* effect is less pronounced in longer alkyl chains relative to 1,2-difluoroethane. This emerged from a study[23] comparing the relative energies of the conformers of *erythro*- and *threo*- 2,3-

10.1002/chem.202000178

difluorobutane, where the energy of several conformations are very close to iso-energetic and there was no obvious outcome to suggest that the extended linear conformation for the *threo* isomer will dominate at all. The significant stability of the *threo* over the *erythro* isomer in these fatty acids, or for the long chain alkyls **13** and **14**, most probably has its origin in optimal macromolecular packing interactions in the solid state, which override weak conformational biases in the isolated molecules. It can be anticipated that the organisation of intermolecular dipolar interactions for each isomer, between the polarised hydrogens and fluorine (HC-F···H-CF), will be significant here in assembly and solid state packing. The importance of intermolecular interactions between the geminally polarised hydrogens and the fluorines of -CHF- groups is very obviously contributing to the high melting points of the more ordered all-*syn* tetra and hexafluoro cyclohexanes that will be considered later, and is emerging here in these long chain alkyls.

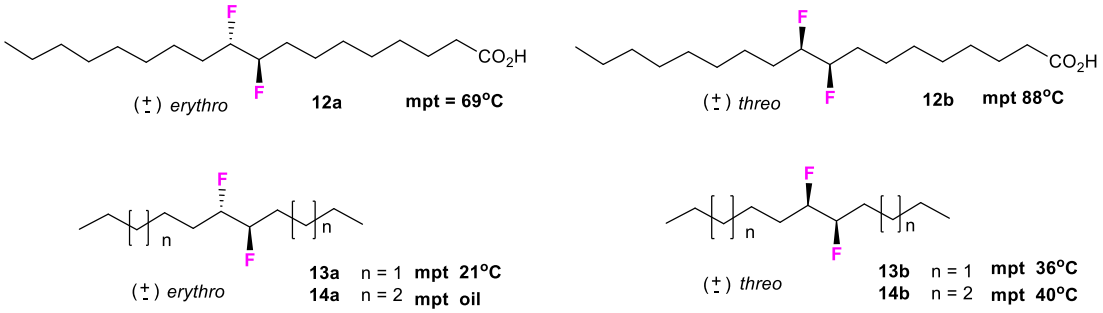

Figure 4 Structures and melting points of the *erythro*- and *threo*- 9,10-difluorostearic acids **12** and selected vicinal difluoro alkanes **13** and **14**.

The observation that diastereoisomers of vicinal difluorides can influence properties led us[26] and others[27,28] to explore the conformation of peptides carrying *erythro* and *threo* vicinal fluorines. Specifically we prepared the dipeptide stereoisomers **15a-c**, with a 2,3-difluorosuccinate core.[26] It was immediately apparent from X-ray structure analysis and solution NMR that these diastereoisomers adopt significantly different conformations as illustrated for the X-ray structures in Figure 5. In each case a *gauche* relationship between the vicinal fluorines is maintained across the central C-C bond. It is also notable that the C-F bonds align *syn* planar to the N-H bonds of the adjacent amides. This is a clearly favoured geometry which arises from dipolar relaxation between the C-F bond and the *anti*-parallel amide carbonyl, as well as an electrostatic attraction between fluorine and N-H hydrogen.[29] It places a significant constraint on the conformation of the amide and the nearest C-F bond, leaving the

10.1002/chem.202000178

central C(F)-C(F) bond freer to rotate. The evidence indicates that this rotation favours *gauche* relationships between the vicinal fluorines.

10.1002/chem.202000178

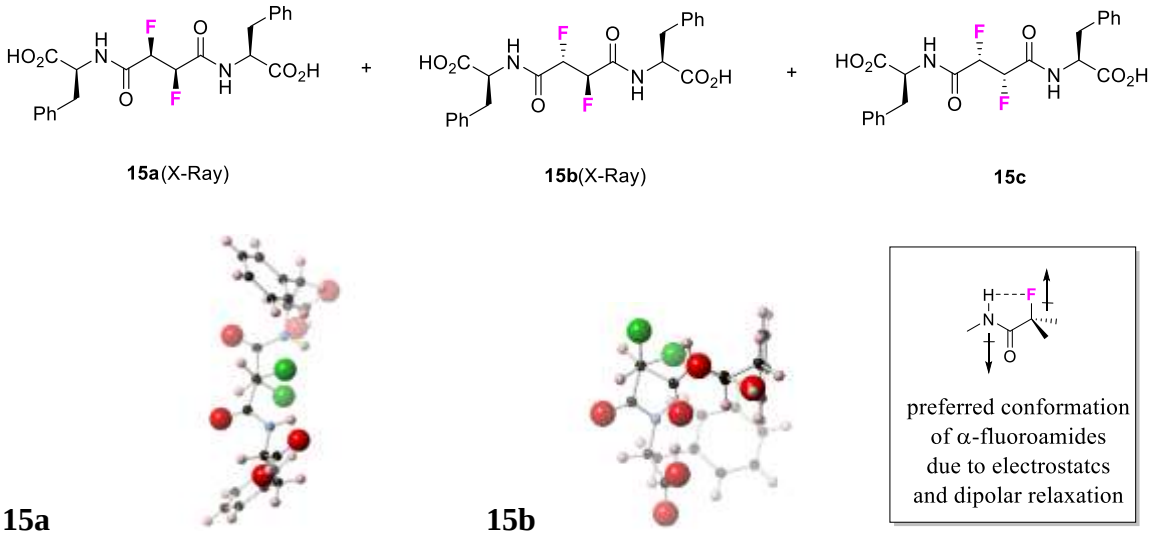

Figure 5. Vicinal difluoro stereoisomers of 2,3-difluorosuccinate diamides **15a-c** adopt different conformations.

These fluorine induced constraints have been used by Hunter who has explored the incorporation of vicinal 2,3-difluorinated stereoisomers of the neurotransmitter γ-aminobutyric acid (GABA)[30] in various situations to try to influence molecular conformation. In a most recent study[28] the 2,3-difluoro-GABA stereoisomers were incorporated into RGD peptides **16a-d**, to generate diastereoisomers differing only by placing a particular vicinal-difluoro stereoisomer into the backbone of the parent RGD peptide. Cyclisation of the linear peptide precursors was significantly influenced by the relative stereochemistry of the fluorines, indicating that the fluorines dictate favoured or less favoured conformations to facilitate cyclisation. Solution state NMR data were used to place constraints in molecular dynamics simulations, and this indicated that the different diastereoisomers (changing the configuration at fluorine only) dictate different conformations of this cyclic peptide, despite it being a small cyclic structure. The fluorines consistently align *gauche* rather than *anti* to each other, however it is unlikely for such a small cyclic peptide that these conformations are dictated entirely by the stereoelectronic *gauche* effect, which is a weak effect. The most significant fluorine effect here is the tendency[29] of the C-F bond at C-2 to align *syn* to the C-1 amide NH and *anti* to the adjacent carbonyl as discussed above (Fig 5). This is achieved in structures A and D but not for B and C. Such studies demonstrate that the relative stereochemistry of vicinal fluorines offers a tool which can influence the conformation of bioactives, even if a particular outcome is difficult to predict.

10.1002/chem.202000178

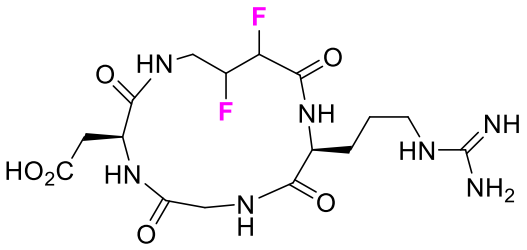

16a-d

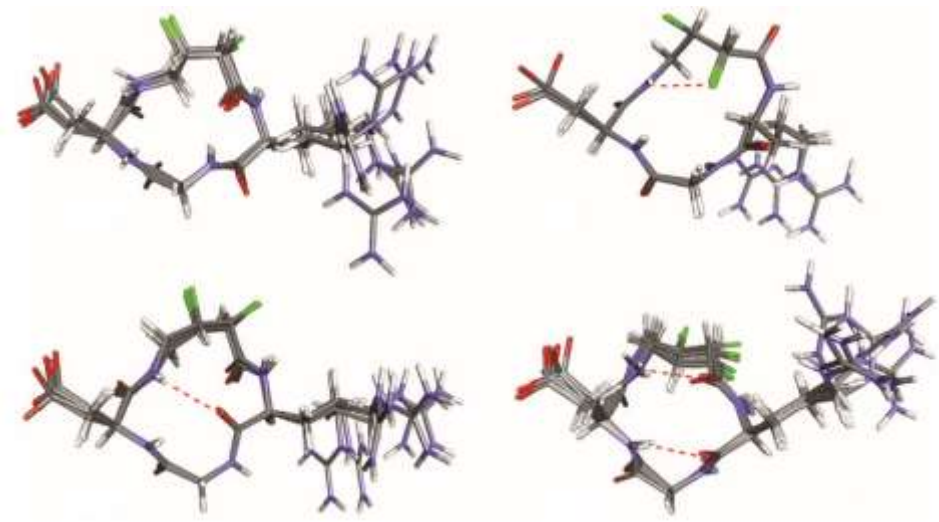

Figure 6. Average conformations of cyclic RGD peptides **16a-d**, incorporating different stereoisomers of 2,3-difluoro GABA, from molecular dynamics simulations informed from solution state NMR coupling constants. [28]

There have been notable recent developments in the synthesis of vicinal difluorides in one step reactions directly from olefins as summarised in Figure 7. These developments built on a reaction originally disclosed by Yoneda's lab,[31] who in 1998 demonstrated that vicinal difluorination of olefins such as cyclohexene **18**, could be achieved with stochiometric *p*-iodotoluene difluoride **17** and $Et_3N.5HN$ as shown in Figure 7(a). In 2016 two papers appeared simultaneously from the Jacobsen[32] and Gilmour[33] labs respectively, demonstrating catalytic protocols for this reaction. The catalytic cycle requires oxidation of iodotoluenes **17** and **20** respectively for turnover. In Jacobsen's case *m*CPBA was used as the oxidant and with pyr.9HF as a fluoride source, whereas the Gilmour protocol used Selectfluor, both as an oxidant and as a source of electrophilic fluorine, along with HF in various organic amine combinations. These

10.1002/chem.202000178

protocols are summarised in Figure 7(b). In many of these reactions high diastereoselectivities are obtained, generally with an overall *syn* addition to the double bond, however *anti* outcomes arise when neighbouring groups participate in anchimeric assistance. Subsequently both laboratories have disclosed enantioselective catalytic difluorination protocols using catalysts **26** and **27** respectively.[32b, 33b] Most recently a highly efficient electrochemical oxidation (of *p*-iodotoluene **23**) process has been disclosed by Lennox[34] which enables vicinal difluorides such as **29** to be prepared without a chemical oxidant. This latter process, illustrated in Figure 7(c) has been manipulated to achieve partitioned protocols which are particularly useful for the preparation of vicinal difluorides of electron rich olefins such as **28** that are easily oxidised and need to be isolated from the electrochemical process. It is method developments such as these which will enable vicinal difluoride stereoisomers to be explored much more widely in bioactives and materials chemistry research programmes.

10.1002/chem.202000178

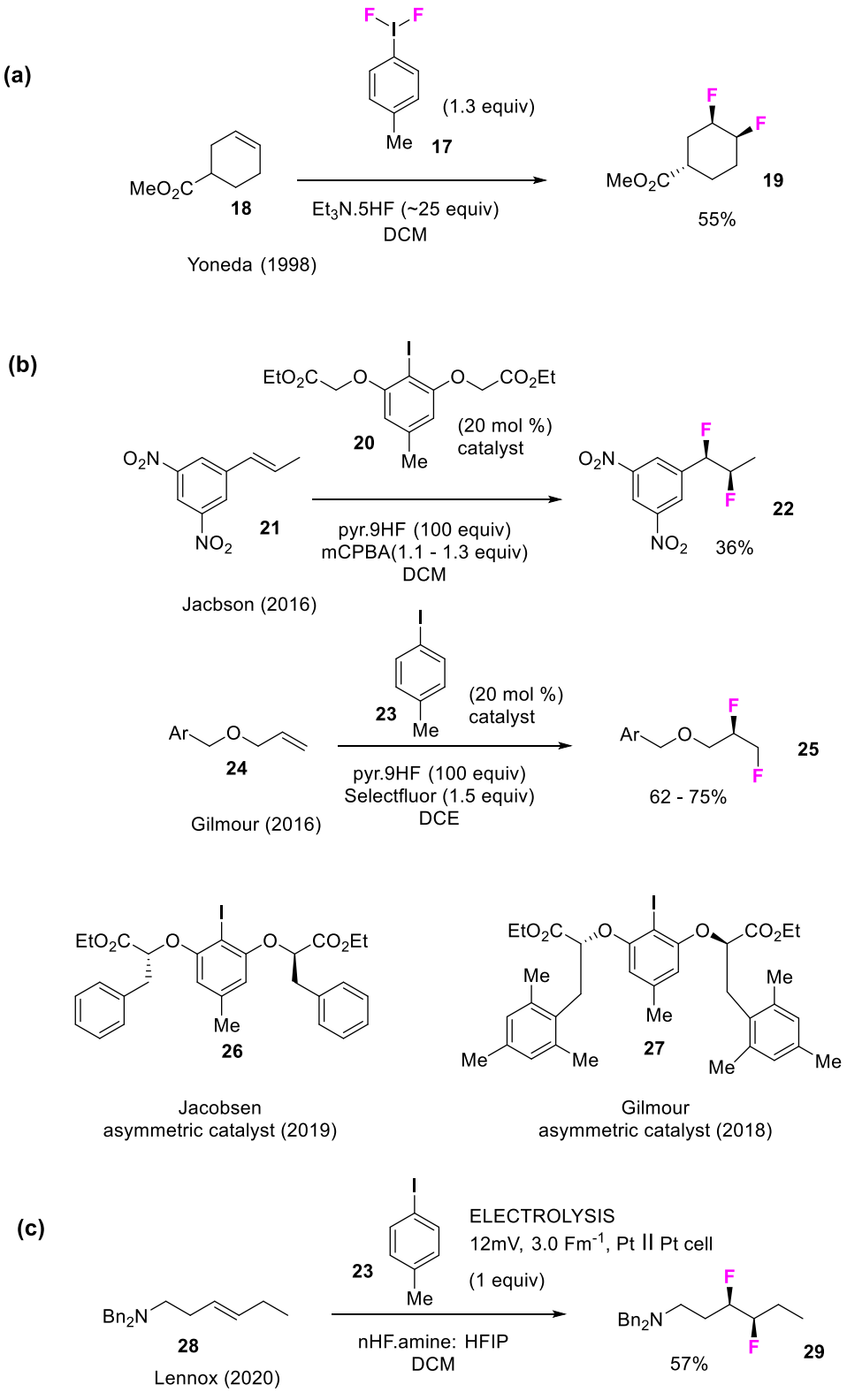

Figure 7 Progression of direct vicinal difluorination methods developing from Yoneda's initial iodotoluenedifluoride **17** treatment of olefins. Selected examples are shown from the catalytic, enantioselective methods and electrochemical methods which have been disclosed recently.[31-34]

10.1002/chem.202000178

Multi-vicinal fluorinated chains

A natural progression from the vicinal 1,2-difluorides led us to prepare compounds with three,[14] four,[15] five[16] and six[17] vicinal fluorines along the alkyl chain, all with defined stereochemistry. The syntheses of these compounds has been reviewed previously[13] and will not be revisited here however key structures are illustrated in Figure 8. A significant effect in determining the overall conformation of such alkanes is an electrostatic repulsion between the fluorines located 1,3- to each other. Conformational analysis particularly of the tetrafluoro-alkanes **33** and **34** revealed that in the solid state and in solution, that these compounds adopt conformations which avoid parallel alignments of 1,3 C-F bonds.[15] This is most dramatically observed in the 1,2,3,4,5,6-hexafluoro systems **37a** and **37b**, where X-ray structures show that isomer **37b** adopts a linear *anti* zig-zag conformation, whereas isomer **37a** has a twisted helical conformation.[17] These conformations are consistent with the avoidance of 1,3 C-F bond alignments and they also accommodate weaker, stabilising stereoelectronic, antiperiplanar C-H(σ) to C-F(σ*) alignments along the backbone, reinforcing *gauche* alignments the between vicinal fluorines.

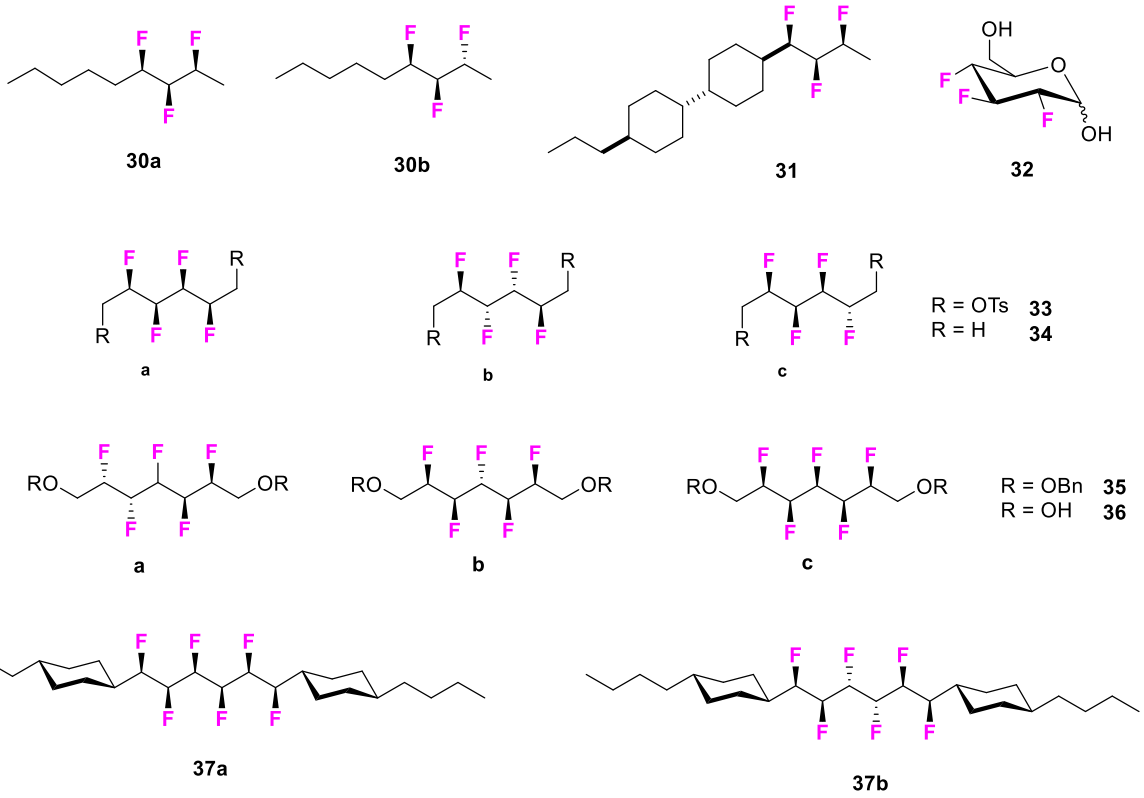

10.1002/chem.202000178

X-ray structure of **37a** (helical) X-ray structure of **37b** (*anti* zig-zag)

Figure 8: A selection of multivicinal fluorinated alkane stereoisomers which have been prepared with three to six fluorines, including the X-ray structures of **37a** and **37b**.

It became an aspiration to try and achieve molecular arrangements that maximise polarity, rather than minimise polarity by allowing the fluorines to turn away from each other. Such arrangements would be desirable for the design and preparation of soft performance materials such as liquid crystals for displays where molecules are designed such that their molecular dipoles are orientated either along or perpendicular to the long molecular axis. This is not obviously achievable in linear chain systems where the main chain, C-C bonds, are free to rotate; however some progress in this direction was achieved recently in a linear chain system with the skipped all-*syn* hexafluoro alkane **54**.[35] The synthesis of **54** is shown in Figure 9 and is discussed in detail in the primary publication. The approach employed many of the strategies for introducing fluorine that had been developed for the preparations of linear alkanes **33**, **34** and **37**. A key aspect too is the metathesis reaction, in this case involving a self-coupling of **50** to generate **51**. Since **50** was prepared in an enantiomerically enriched form, then the coupled product is a single stereoisomer (enantiomer) of high stereochemical purity.

10.1002/chem.202000178

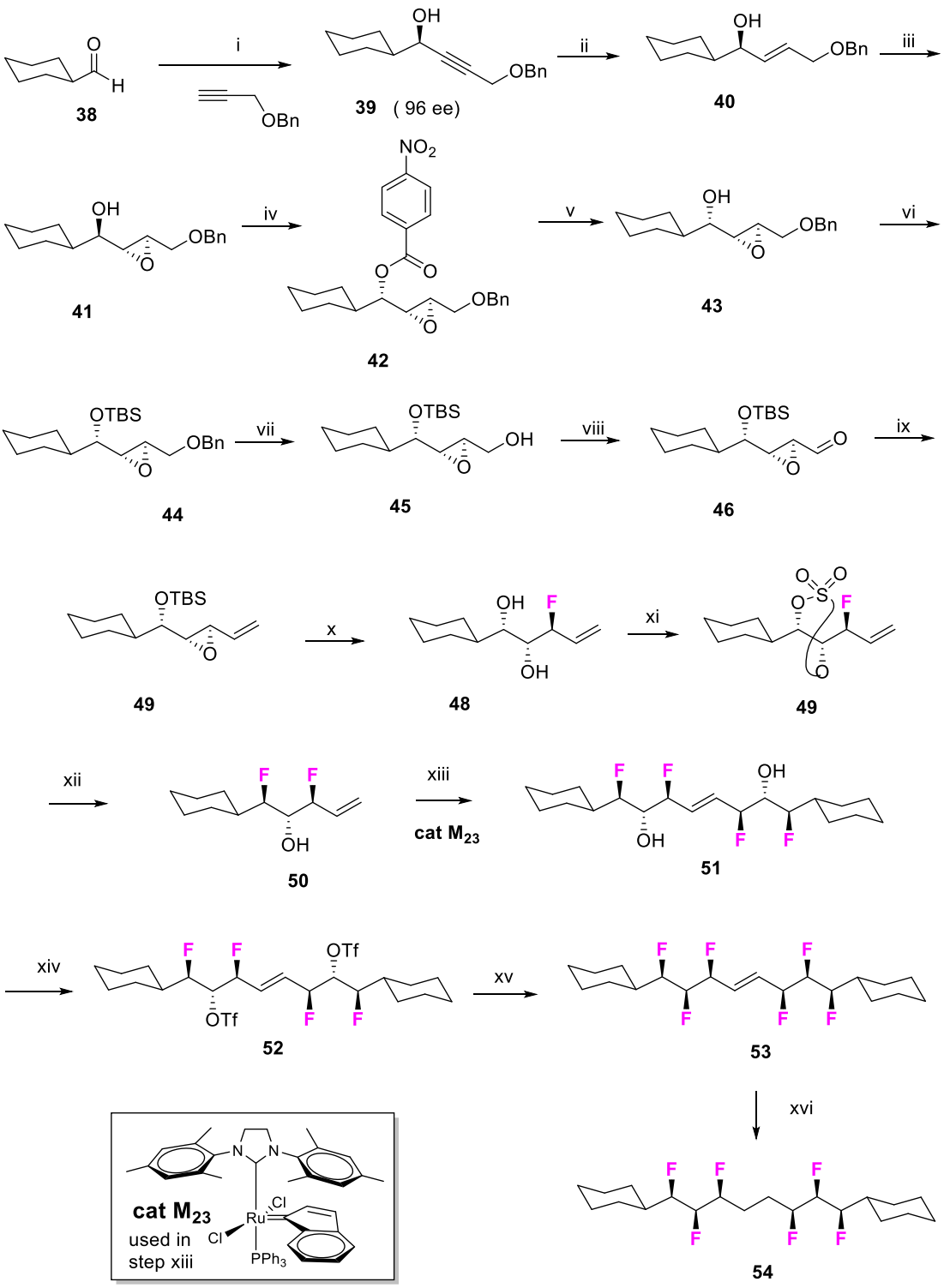

Figure 9: i) $Zn(OTf)_2$, (+) *N*-Methylephedrine, Et_3N, Tol., reflux, 16h, 88%; ii) Red-Al, THF, - 40 °C, 5 hrs, 92%; iii) $Ti(OPr\text{-}i)_4$, (-) diisopropyltartrate, *t*-BuOOH (0.8), 4Å MS, DCM, - 40 °C, 4 d, 72%; iv) *p*-nitrobenzoic acid, DEAD, PPh_3, THF, 0 °C then rt 16h, 63%; v) K_2CO_3, MeOH, rt, 2 hrs, 97%; vi) TBSOTf, Py, rt, 16h, 95%; vii) H_2, 10% Pd/C, MeOH, rt, 16h, 92%; viii) Dess-Martin periodinane, Py, DCM, rt, 16h, 80%; ix) $MeP(Ph)_3$ Br, KHMDS, THF, -10 °C; 93%; x) 0 °C, $Et_3N.3HF$, 120 °C, 16h, 82%; xi) SO_2Cl_2, Et_3N, DCM, -78 °C then -10 °C, 85%; xii) $Et_3N.3HF$, 110 °C, 16h, 18%; xiii) Catalyst M23, DCM, rt, 5 day, 59%; xiv) Tf_2O,

10.1002/chem.202000178

DCM, rt, 3d, 95%; xv) Et_3N,3HF, Et_3N, 50 °C, 4h; xvi) H_2, 10% Pd/C, MeOH, rt, 16h; (80% steps over last two steps).[35]

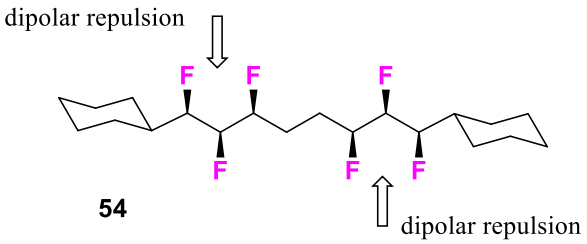

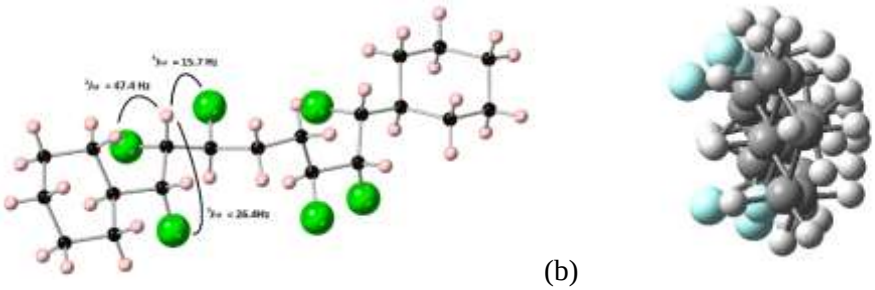

Figure 10. The conformation of the trifluoromotifs of **54** are helical due to 1,3-difluoro repulsion. (a) X-ray structure indicated a continuous helix. (b) DFT computation suggest the fluorines align along one face of the fluorines inducing a high molecular dipole (μ = 7.15 D).[35]

This molecule (**54**) has an ethylene bridge with two fluorines missing from a complete linear array of eight. In the solid state (see X-ray structure in Figure 10(a)) a helical structure was maintained across the non-fluorinated ethylene bridge however in solution is was apparent that there was a significant conformational dynamic across the hydrocarbon bridge, although the all-*syn* trifluoro motifs held their helical integrity, as judged by $^3J_{HF}$ coupling constants (Figure 10(b)). A DFT computational evaluation identified the complete helical structure as a low energy structure. Interestingly this structure had a very high molecular dipole (μ = 7.11 D), and the X-ray and optimised computational structure reveals that all of the fluorines run along one side of the molecule. The two 'missing' fluorines would orient to the opposite face and their polarity would counter and minimise the overall molecular dipole. The lowest energy structure identified had an *anti* zig-zag conformation across the ethylene bridge, and had a very low molecular dipole (μ = 1.01D) , however this was almost iso-energetic with the polar helical structure, and thus the polar conformer should be a significant one in solution. It follows that

10.1002/chem.202000178

there may be an advantage for the preparation of liquid crystalline compounds or polar polymers, to have sequences of three all-*syn* fluorines followed by a two methylene spacer, to create polarity in solution.

Gilmour's lab has recently[36] demonstrated significant solubility differences, as well as selected pharmacokinetic properties, between stereoisomers of the linear tetrafluoroalkyl ethers **55a** and **55b** shown in Figure 11, which are close analogues of the multiple sclerosis drug Gilenya, demonstrating that the arrangement of the fluorines significantly influences the physiochemical chemical properties of linear alkanes.

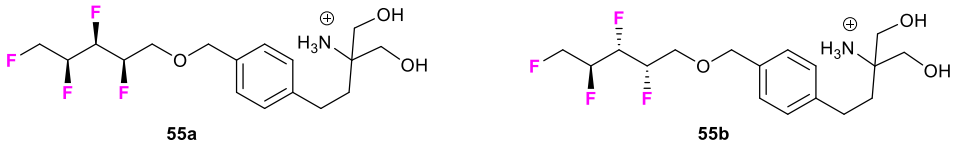

Figure 11: Tetrafluoroalkane stereoisomers, display different physiochemical properties.

In order to generate conformationally constrained, highly polar compounds of this class, it became obvious that rings were required to encourage C-F bonds to co-align. Thus a research objective to prepare rings with vicinal fluorines arranged on one face of the alicycle emerged. The most obvious ring size in this context is cyclohexane[18-20] where C-F bonds could be positioned to adopt 1,3-diaxial arrangements in chair conformations, and this formed a focus of our research programme, however in this campaign we have also prepared a cyclopentane[37] of this class and most recently a preparation of the all *syn* 1,2,3-trifluorocyclopropane motif[38] was developed for the first time.

Selectively fluorinated cyclohexanes.

At the outset, the literature on selectively fluorinated cyclohexanes was relatively sparse. Some relevant structures are illustrated in Figure 12. Monofluorocyclohexane **56** is well known and has been prepared in the context of establishing the A (axial)-value for fluorine. Fluorine has the lowest A-value (0.24 – 0.42 kcal mol^{-1}) after the isotopes of hydrogen.[39] This is entirely consistent with the dogma that fluorine is the next smallest atom available in chemistry that can form a stable covalent bond to carbon. Perhaps more interesting in the context of the current discussion are the *syn* stereoisomers of 1,2 **57**; 1,3 **58** and 1,4- **59** difluorocyclohexanes. In the case of 1,2- difluorocyclohexane **57** the *syn* isomer interconverts between isoenergetic conformers.

10.1002/chem.202000178

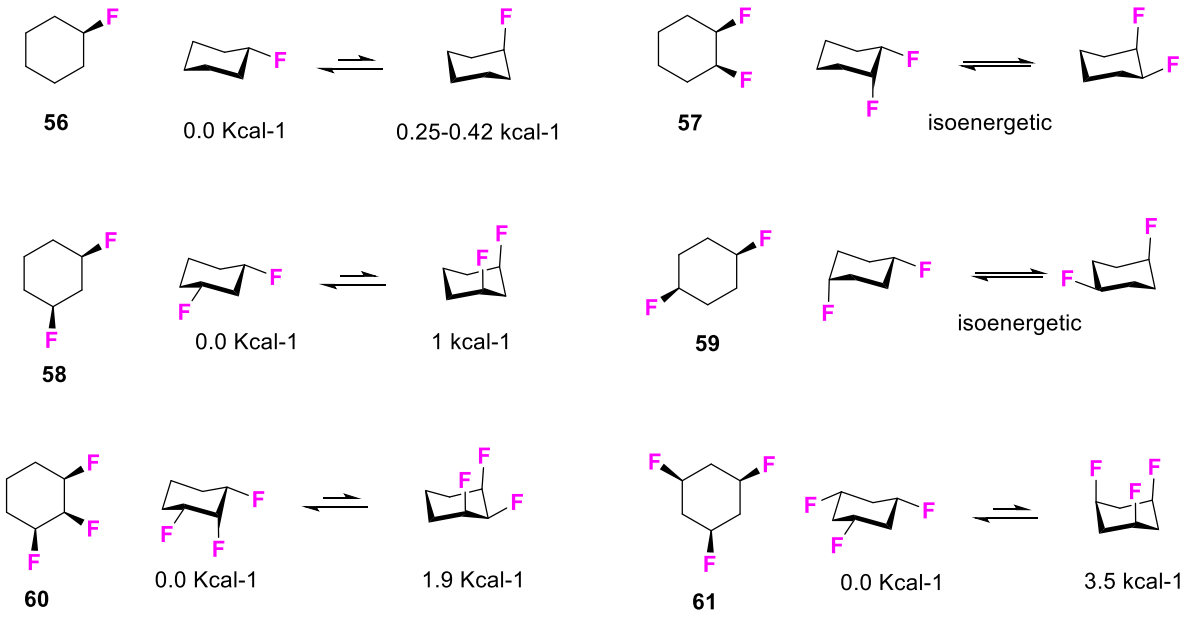

Figure 12: Calculated relative energies in the gas phase[40] of ring interconverted all-*syn* di- and tri- fluorinated cyclohexanes **56**-**61**.

The 1,3- **58** and 1,4- **59** difluorocyclohexanes have never been reported experimentally although theory suggests[40] that the 1,3- diaxial conformer of **58** suffers from electrostatic repulsion between the fluorines, and thus the diequatorial isomer is predicted to be lower in energy. The energy difference (gas phase) is only around 1.0 kcal mole, suggesting some stabilisation of the axial C-F bonds by C-H(σ) to C-F(σ*) HOMO-LUMO interactions. Interconversion of the *syn*-1,4-difluorocyclohexane **59** again leads to isoenergetic structures.

For the various possible isomers of trifluorocyclohexane only two have been prepared experimentally. These are all-*syn* 1,2,3- and all-*syn* 1,3,5- trifluorocyclohexane **60** and **61**. These syntheses were achieved by the Glorius lab in their recent direct hydrogenation of the corresponding trifluorobenzenes,[41] but no experimental data has been presented on their preferred conformations, which are non-equivalent after ring inversion in each case. Theory (gas phase) calculations[40] for **60** predict that the *eq, ax, eq* conformer is favoured over the inverted *ax, eq, ax* conformer by around 1.9 kcal mol^{-1}, again indicative of 1,3 diaxial repulsions between the axial C-F bonds and where the less polar isomer will predominate. The all *syn* 1,3,5 triaxial conformer of **61**, with a triangular arrangement of three axial C-F bonds is calculated to be significantly higher in energy (~3.5 kcal mol^{-1}) than the all equatorial conformer. The all-axial conformer has a very high molecular dipole (μ = 5.7 D) however if

10.1002/chem.202000178

prepared, theory suggests that the significantly less polar (μ = 1.67 D) all equatorial conformer of **61** will dominate in solution making this a less interesting target molecule.

Our first entry into vicinal multifluorinated cyclohexanes addressed the all-*syn* tetrafluoro isomers **64** and **65** of cyclohexane.[18] These were the first fluorinated cyclohexanes of this tetrafluoro class to be prepared and they are distinguished in that they cannot avoid a ground state chair structure containing polar 1,3-diaxial C-F arrangements. Such a feature was anticipated to impart a significant polarity to the cyclohexane ring unlike the conformationally free open chain systems described above. The synthesis of **64** and **65** was accomplished from *syn* diepoxide precursors **62** and **63** respectively as summarised in Figure 13. In the case of **64** a sequential approach was taken, however **65** was prepared much more directly by a DAST reaction on the precursor diepoxide **63**. This was accomplished in a 24% yield after 3 days at 70 °C (care has to be taken as DAST is explosive - detonation temperature =144 °C). More recently these compounds have been prepared by the direct hydrogenation of the corresponding tetrafluorobenzenes.[37]

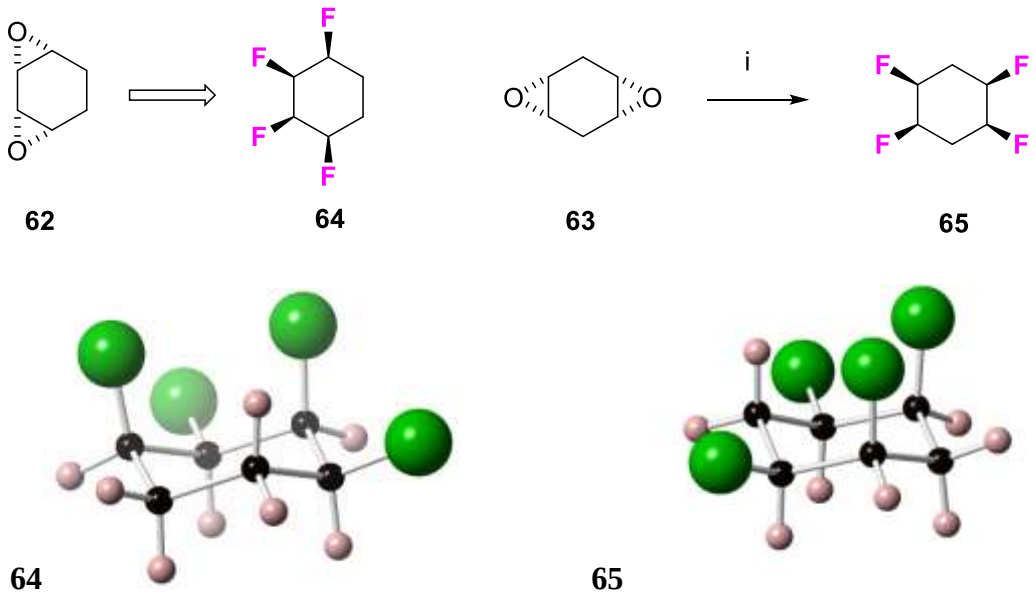

Figure 13: X-ray structures of all-*syn* tetrafluorocyclohexanes **64** and **65** showing 1,3-diaxial C-F bond relationships in the chair conformations. Conditions i. DAST (neat), 70 °C, 72h, 24%.[18]

Cyclohexanes **64** and **65** are both white crystalline solids (mp 83 °C for **64**; mp 109 °C for **65**), perhaps surprising for cyclohexanes with only four fluorines. They are crystalline due to their

10.1002/chem.202000178

unusually high molecular dipole moments, which arise from 1,3-diaxial C-F bond alignments a feature that is obvious in their X-ray structures (Fig 13). In both cases crystal packing is such that the fluorine face of one ring contacts the hydrogen face of another due to electrostatic ordering. Informative experiments, which report the facial polarity of these rings were conducted by recording ^{1}H-NMR spectra in $CDCl_3$ and then in toluene.[18] The toluene ring associates parallel, through FC-H…π interactions, with the electropositive (hydrogen) face of these molecules in solution and anisotropically induced shifts occur due to the aromatic ring current. The value of the shifts are disproportionately high for the hydrogens on the electropositive face, with particularly large changes in chemical shift for the axial hydrogens. For the fluorine face HC-F…π repulsion is anticipated to orient the aromatic solvent perpendicular to the cyclohexane and the anisotropic effect is significantly diminished.

1,2,3,4,5,6-Hexafluorocyclohexane

Having made all *syn* tetrafluorocyclohexanes **64** and **65**, it became an objective to prepare an isomer of 1,2,3,4,5,6-hexafluorocyclohexane **66**. There are nine possible configurational isomers of this molecule and a preparation of any one of these isomers requires a unique approach, in order to control stereochemistry.

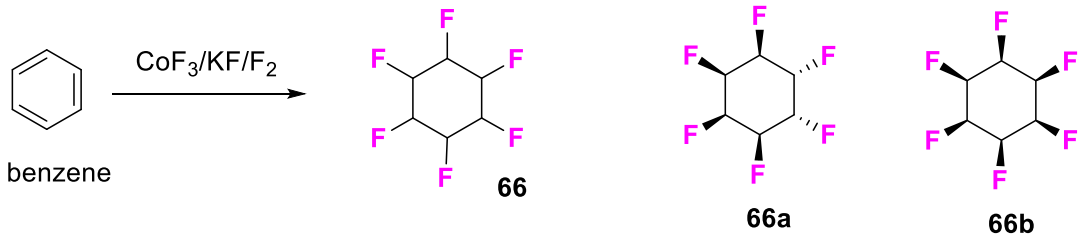

Figure 14: 1,2,3,4,5,6-Hexafluorocyclohexane **66**. Isomers **66a** and **66b** have been synthesised.[19,20,37]

The synthesis of two stereoisomers (**66a** and **66b**) of this class, shown in Figure 14 was achieved in our programme however there was an historical account in the literature from 1969[42] of a 1,2,3,4,5,6-hexafluorocyclohexane which had been isolated as a side product (~2%) of a $CoF_3/KF/F_2$ reaction from benzene, in a study exploring the synthesis of fluorobenzene. Chemical analysis and mass spectroscopy were consistent with a formulae of $C_6H_6F_6$ and low field ^{1}H- and ^{19}F- NMR indicted the presence of CHF groups only. The account concluded that; '*These facts suggest that compound (VII) is a 1,2,3,4,5,6-hexafluorocyclohexane very*

10.1002/chem.202000178

probably with the trans structure.[42] Thus such a compound had most probably been prepared although its stereochemistry, and whether the product was a single isomer, was not clear.

Our first campaign to an isomer of **66** started with **66a**. The synthesis of **66a** is described in detail elsewhere[19] but the route developed from a report in the literature involving the treatment of benzene with AgF_2 to give tetrafluorocyclohexene **67**.[43] This precursor was developed to stereoisomer **66a** which was a crystalline compound and X-ray confirmed the stereochemical configuration (see Figure 15).

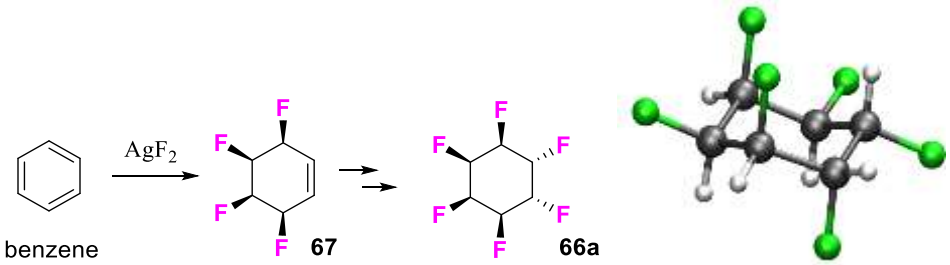

Figure 15: Summarised schematic of the synthesis and X-ray structure of **66a** from benzene.[19]

The room temperature ^{19}F-NMR spectrum of **66a** shown in Figure 16 (a) was rather featureless as the peaks are averages of pairs of fluorine signals that interconvert from axial to equatorial, however on cooling the sample to -80^{o}C (Figure 16b), then all six of the fluorines became non-equivalent due to slow interconversion of the cyclohexane chair conformations at this temperature. This ring interconversion, between enantiomeric chairs, could be followed in an ^{19}F-EXSY NMR experiment (Figure 16 c), which revealed the pairs of fluorines that interconvert from axial to equatorial, due to residual nuclear polarisations.

10.1002/chem.202000178

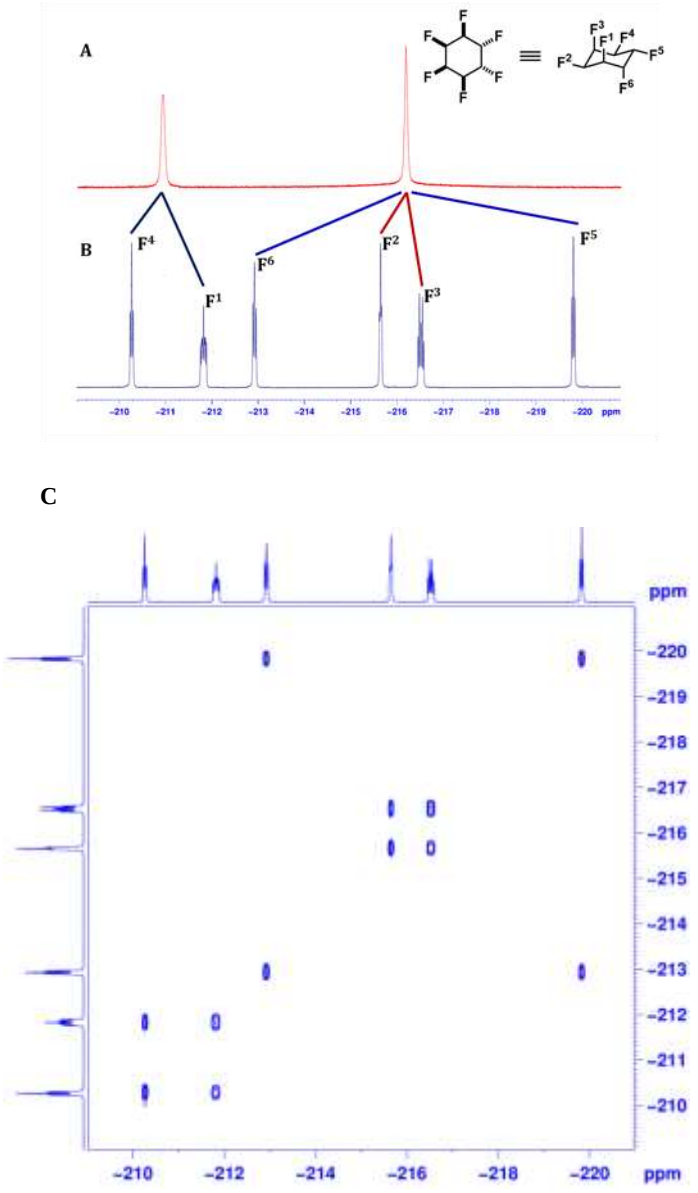

Figure 16: (**A**) Room temperature $^{19}F\{^{1}H\}$-NMR and (**B**) at -70 ºC of **66a** where all the fluorines are resolved. (**C**): 2D-^{19}F-EXSY correlation spectroscopy of **66a** at -70 °C with three sets of correlating peaks indicating the axial/equatorial interconversions with ring inversion.[19]

10.1002/chem.202000178

Isomer **66a** represented one of the nine possible configurational isomers of 1,2,3,4,5,6-hexafluorocyclohexane. The energies of all of these isomers have been calculated in several studies,[40] and **26a** is a relatively low energy isomer. The most interesting isomer in this regard is the all-*syn* 1,2,3,4,5,6-hexafluorocyclohexane **66b**. Theory predicted that this was highest in energy around 15 kcal mol^{-1} above the most stable configurational isomer. This can be accounted for primarily due to the necessary triaxial C-F bond arrangement in the ground state chair conformation of **66b**. The calculated molecular dipole is around 6.2 D, very high for an aliphatic, and thus this most polar isomer became an obvious synthetic target.

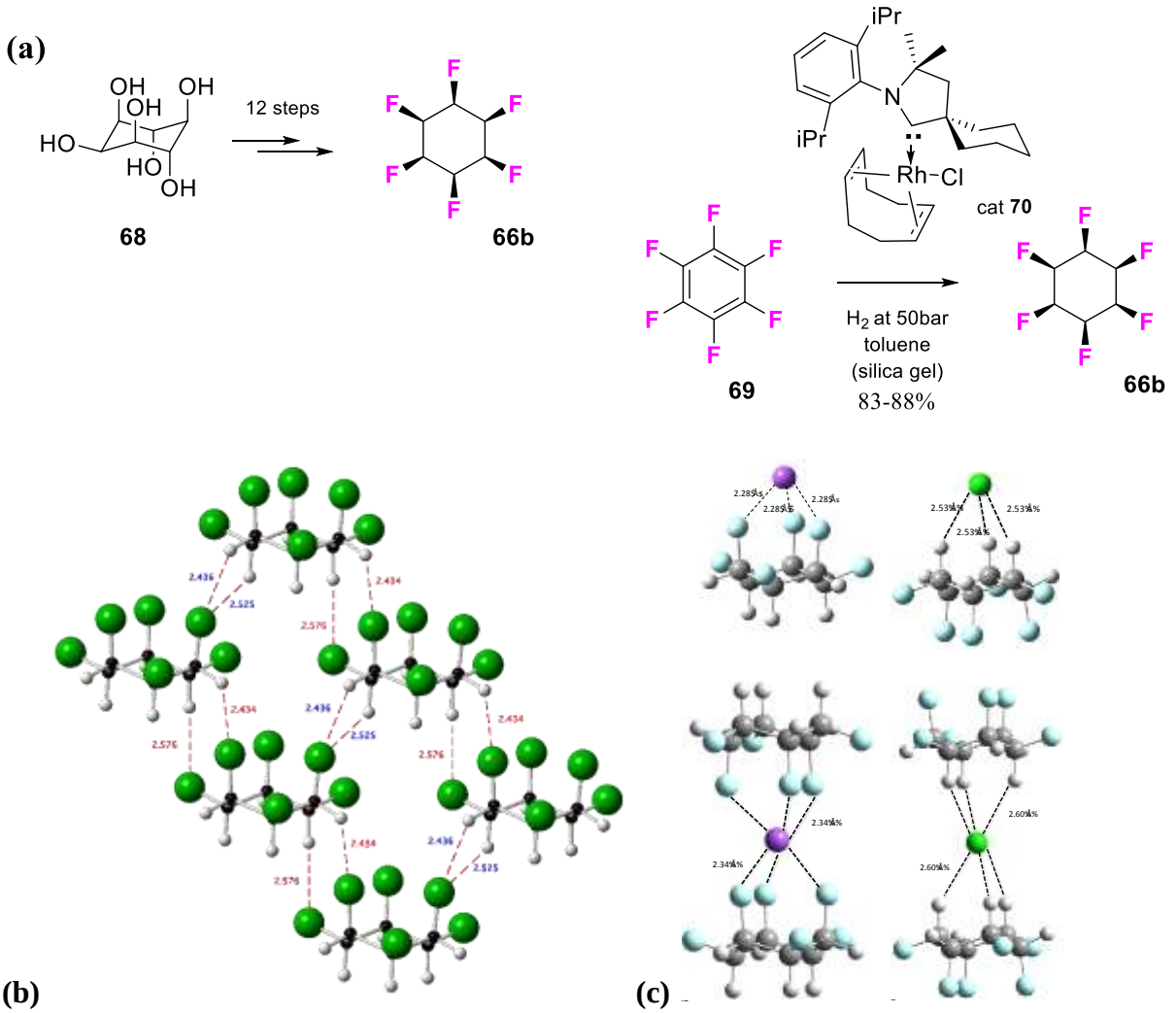

Figure 17: (a) A summary of the first[20] and subsequent syntheses[41] of **66b**. (b) The crystal structure and electrostatic ordering of the packing of **66b**.[20] (c) Optimised structures of **66b** coordinated with either Na^+ or Cl^- as 1:1 and 2:1 complexes.

Our approach to **66b** envisaged starting from a stereochemically defined cyclohexane with an oxygen on each carbon. Accordingly the route that was developed started from inositol **68** as

illustrated in Figure 17(a) and is described in detail elsewhere.[20] The route was significantly improved in 2017 by the Glorius laboratory who reported[41] a one step synthesis of **66b** by direct hydrogenation of hexafluorobenzene **69**. This reaction had always been a prospect but does not work with standard hydrogenation catalysts. The successful hydrogenation required a high pressure (50 bar) hydrogenation using the rhodium, cyclic alkyl amino carbene (CAAC) NHC catalyst **70**, a catalyst which had been developed by Zeng in 2015 for aryl hydrogenations more generally[44] (Figure 17 (a)). Optimisation of this reaction, and with the addition of silica gel as a suitable reaction surface, resulted in a direct transformation of **69** to **66b** in greater than 80% yield, a very significant improvement on the original synthesis. The process was exemplified to offer a range of all-*syn* multivicinal fluorocycloalkanes including the all-*syn* tetrafluorocyclohexanes **64** and **65**, and it was most recently extend to the hydrogenation of aromatic N-heterocycles to generate fluoro-piperidines and related heterocycles.[45] Thus, this direct hydrogenation reaction has opened up access to a wide range of multivicinal fluoro-alicyclic and hetero-alicyclic building blocks for exploration in different arenas of discovery chemistry.

The extraordinary high melting point of **66b** (208 ^{o}C dec.) was immediately noteworthy, consistent with its high polarity, and an image of the X-ray structure of **66b** is illustrated in Figure 17(b). The individual molecules pack one above another, with the fluorine faces contacting the hydrogen faces of the next molecule consistent with an electrostatic ordering, as already observed in the all *syn* tetrafluorocyclohexanes **64** and **65**. Highly unusual for an aliphatic, cyclohexane **66b** binds both cations and ions to its complementary electrostatic faces. The structures of such complexes were explored in the gas phase, initially by the isolation of sodium (Na^+) ion and chloride (Cl^-) ion complexes in a mass spectrometer ion chamber. IR spectra were then recorded by passing a free electron laser through the ion chamber, and the data was used in combination with theory to determine the structure of these ions.[46] In each case 1:1 or 1:2 complexes could be isolated and spectroscopy recorded. The structures of computationally optimised cation (Na^+) and anion (Cl^-) coordinated structures are illustrated in Figure 17(c) where the ions sit symmetrically above and below the faces of the cyclohexane ring.[46(a)] Certain features of the structures emerge. For the Cl^- 1:1 complex both the axial and equatorial C-F bonds lengthen relative to a noncomplexed structure, however for the 1:1 Na^+ ion complex the axial C-F bonds lengthen, and the equatorial C-F bonds shorten relative to the noncomplexed cyclohexane, consistent with electrostatics. In solution, affinities (values in acetone as a solvent) to F^- (K_a = 600 ± 400 M^{-1}) , Cl^- (K_a = 400 ± 40 M^{-1}), Br^- (K_a = 150 ± 7 M^-

^{1}) and I^{-} (K_a = 37 ± 7 M^{-1}) have been measured for **66b** with association constants (K_a) of ~10^2 recorded in each case, and with the highest affinities for fluoride and chloride ion.[47] It should be noted however that fluoride acts as a base and resulted in dehydra-halogenative degradation of **66b**. Subsequently there have been theory studies[48] exploring ion affinities of **66b** across a wide range of metals and there has been a focus on exploring the **66b** ring system and derivatives as candidate components in non-linear optical devices.[49]

All-*syn* 3-aryl-1,2,4,5-tetrafluorocyclohexane building blocks

It became an objective to introduce these all-*syn* selectively fluorinated cyclohexanes into building block for drug discovery, as such a Janus face motif has no obvious counterpart in that arena. For our part we explored the synthesis of a range of aryl- all-*syn* tetrafluorocyclohexanes as candidate building blocks. This has been facilitated by the ready availability of phenylcyclohexane **71**, which can be prepared on a multigramme scale.[50] It is interesting to observe in the X-ray structure of this aryl derivative that the phenyl ring of one molecule associates with the electropositive face of the cyclohexane ring as shown in Figure 18. This illustrates a potential binding mode for pharmaceutical candidates to aromatic amino acid residues. Conversely the fluorine face should be attracted to positively charged side groups as well as protein bound metal cations as previously illustrated in Figure 17(c).

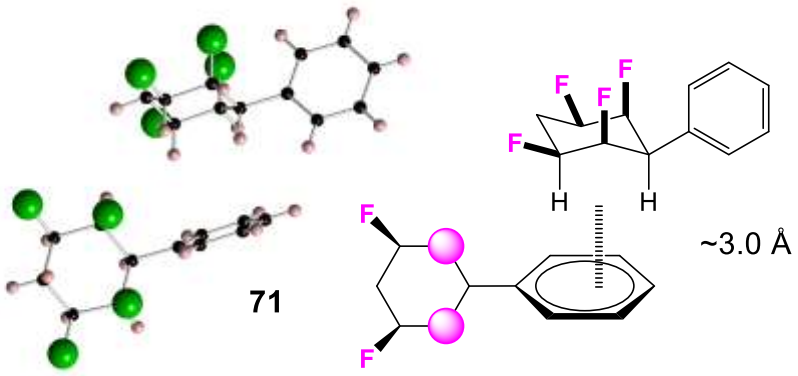

Figure 18: X-Ray structure of **71** illustrating an intermolecular interaction between the phenyl ring and hydrogen face of the cyclohexane ring.[50]

Electrophilic aromatic substitutions reactions of **71**[50b] are not so selective and tend to afford almost equal mixtures of *o*-, *m*- and *p*- products as illustrated for nitration in Figure 19, to give isomers of **72a-c**. However these can generally be separated by chromatography. In this way nitration, followed by reduction leads to anilines **73b** and **73c**. The *para* aniline **73c** could be

10.1002/chem.202000178

separated and was efficiently converted to phenol **74** *via* diazotisation, or pyrrole **75** following a Paal-Knorr approach, or to aryl bromide **76** via a Sandmeyer reaction. Aryl bromide **96** was progressed through a Sonogoshira reaction to the liquid crystalline type compound **77**.

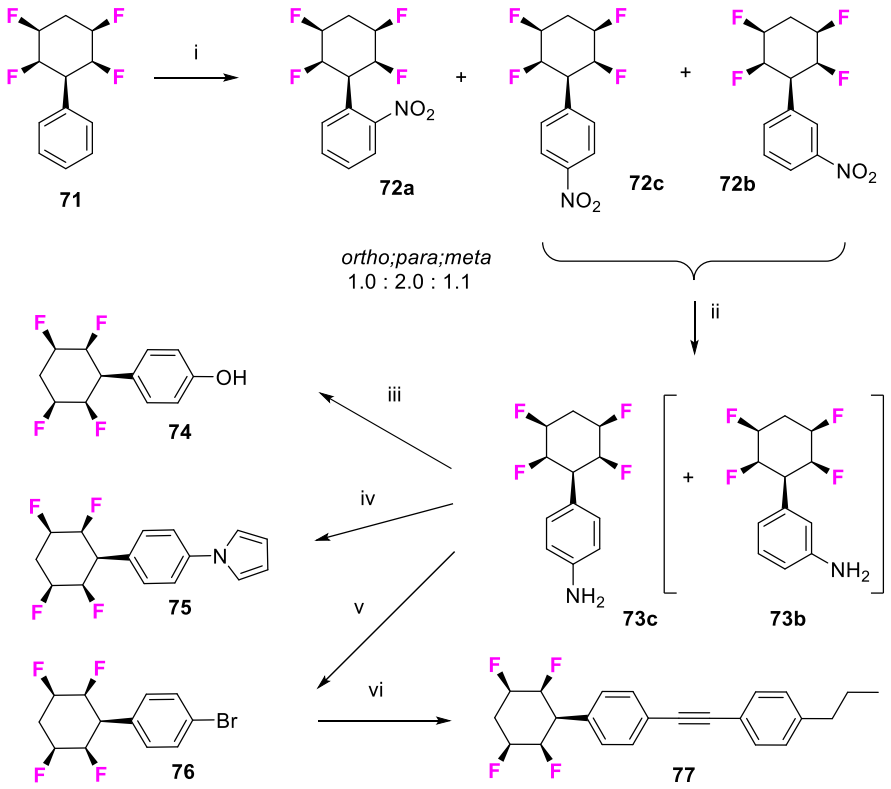

Figure 19: Aromatic building blocks. Conditions; i. HNO_3 (20 eq), H_2SO_4 / $MeNO_2$, rt, 2.5 h, 99%; ii. $SnCl_2$, HCl, EtOH, 80°C, 99%; iii. $NaNO_2$, H_2SO_4, H_2O, 0°C, 83%; iv. $FeCl_3.6H_2O$, 2,5-dimethoxy-THF, THF, H_2O,70 °C, 69%; v. $NaNO_2$, aqHCl, 0 °C then CuBr, aq. HBr, 76%; vi. $PdCl_2(PPh_3)2$, CuI, PPh_3, Et_3N, 80°C, DMF, 87%.[50b]

Iodination of **71** generated the *ortho, meta* and *para* isomers of aryl iodide **78a-c**. As for nitration, the *meta/para* isomers **78b** and **78c** could be separated from the *ortho* isomer **78a** and they were carbonylated (shown in Figure 20 for the *para* isomer only) to generate the corresponding aldehyde **79**, which was progressed to azide **80**, and then through 'click;' reactions to the corresponding amino acid derivatives **81** and **82**.[51] The *meta* and *para* isomers were used to access the corresponding L-phenylalanine derivatives shown only for the *para* isomer **84c** in Figure 20.[52] A Negiishi type coupling on a mixture of **78b/c** with the protected alanyl iodide **83** generated *meta* and *para* products from which **84c** (and separately **84b**) was isolated and then hydrolysis generated the free amino acid **85c**, as confirmed by X-ray structure analysis. This amino acid was progressed to dipeptides from either the N or C terminus, and

10.1002/chem.202000178

was also coupled to penicillin to generate a novel antibiotic dipeptide **88** and **89** as shown in Figure 20.

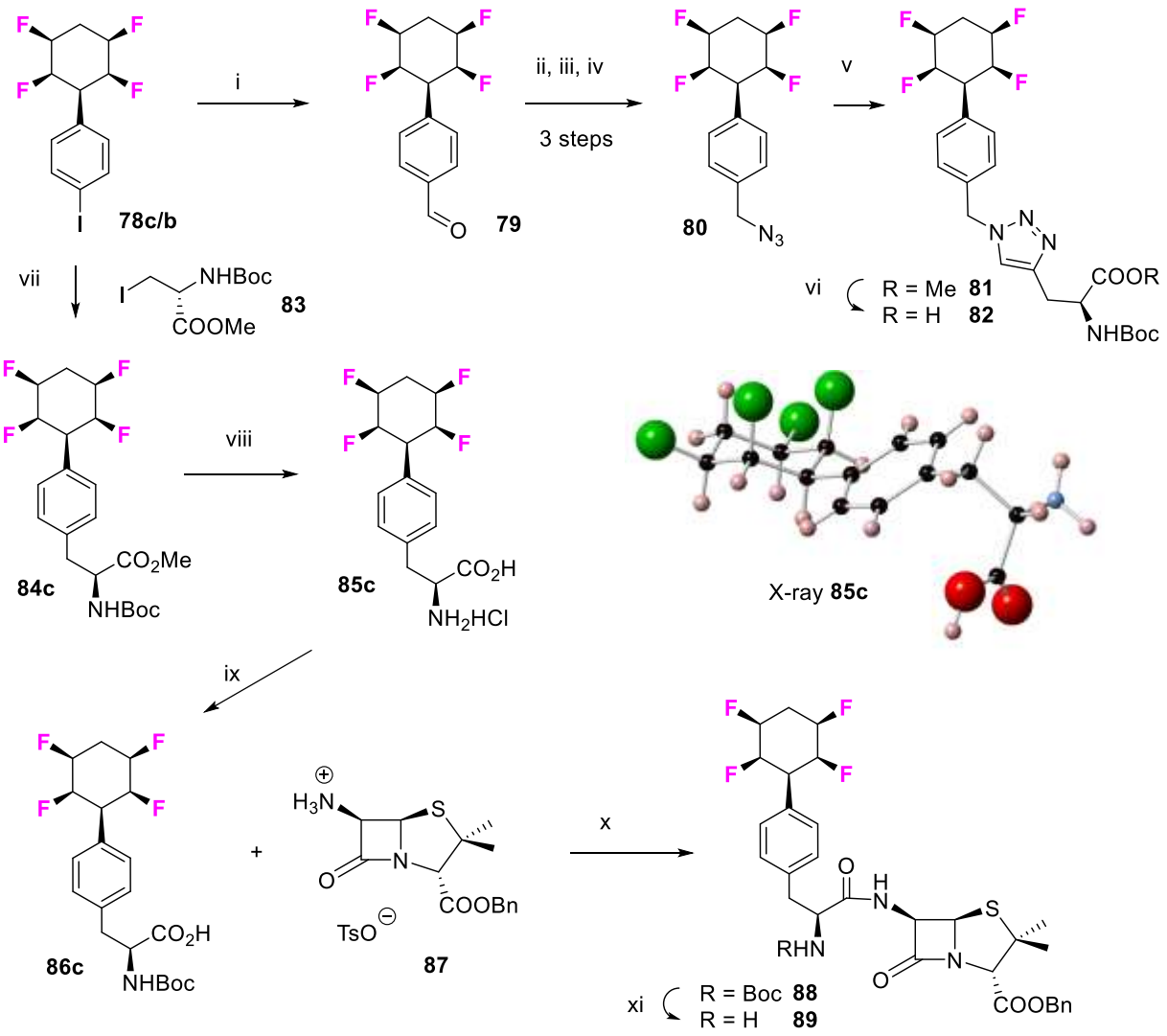

Figure 20: Azide and amino acid building blocks. i. $Pd(PPh_3)_4$, Bu_3SnH, THF, CO (1atm), 50°C, 3h, 70 %; ii. $NaBH_4$, THF, 20 °C, 1h, 98 %.; iii. HI, $CHCl_3$, 30h, 95 %; iv. Bu_4NN_3, acetone / H_2O (4:1), 20 °C, 3h, 94 %; v. acetylene-amino acid; $Cu(OAc)_2$, Na ascorbate, *t*-BuOH, H_2O, 20 °C, 16h, 72 %; vi. HCl (6M), 1,4-dioxane, 80 °C, 48 h, 96 %; vii. Zn, I_2, DMF, **8** ,$Pd_2(dba)_3$, SPhos, 85 %; viii. 6M HCl in 1,4-dioxane, 70 °C, 48 h, 100%; ix. $NaHCO_3$, THF/H_2O (1:1), $(Boc)_2O$, rt, 16h, 93%; x. EDCI, HOBt, DMF, NMM, 16h, 81 %; xi. 4M HCl, 1,4-Dioxane (1:1), 1 h, 83%.[51,52]

10.1002/chem.202000178

It was attractive to prepare cyclohexane carboxylic acid **90** carrying four *syn* C-F bonds on the ring, as a candidate building block, however any attempt at oxidation of the phenyl ring of **71** to release carboxylic acid **90**, resulted only in dehydrofluorination and further degradation, as illustrated in Figure 21, so this proved unsuccessful. However if the *alpha* carbon of cyclohexane carboxylic acid **90** is capped with a substituent, then such ring systems are stable to hydrogen fluoride elimination, and can be progressed to useful building blocks, by oxidation of the aryl ring.

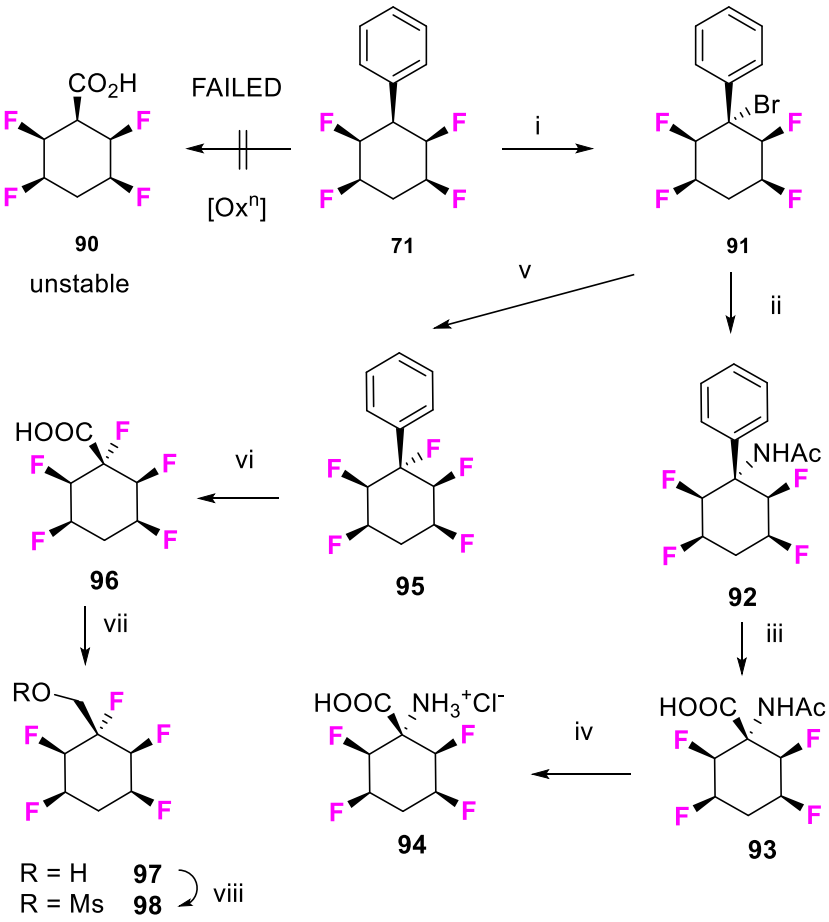

Figure 21: Carboxylic and amino acid building blocks. i. NBS, CCl_4/MeCN (10/1), 100°C, 42h, 89%;%); ii. MeCN, H_2SO_4, 90°C, 48h, 68%; iii. H_5IO_6, 5% $RuCl_3$, H_5IO_6, 5% $RuCl_3$, 90°C, 42h, 61%; iv. 6N. HCl, 16h, 100°C, 55%; v.Ag(II)F, $(C_2H_5)_2O$, 35°C, 20h, 82%; vi H_5IO_6, 5% $RuCl_3$, 90°C, 42h, 74%; vii. BH_3.THF, THF, 16h, 50°C, 55%; viii. MsCl, Et_3N, DCM, 0°C, 0.5h, then RT, 18h, 63%.[53]

The most straight forward procedure here involved direct bromination of phenylcyclohexane **71**, to give **91** as a single diastereoisomer in good yield.[53] This bromide can be progressed in several ways. Treatment in acidic acetonitrile results in a Ritter type process to generate acetamide **92**. The aryl ring of **92** was readily oxidised to carboxylic acid **93**, and then amide

10.1002/chem.202000178

hydrolysis gave the free amino acid **94** as a novel building block. Alternatively, bromide to fluoride exchange of **91** with silver fluoride, to generate **95**, proved to be a straightforward reaction, one that occurs exclusively with a retention of configuration. The newly introduced fluorine at the benzylic position acts as a blocking group and the resultant phenyl pentafluorocyclohexane **95** could be oxidised to carboxylic acid **96**. This carboxylic acid was converted to a range of amides, or alternatively further reduction gave alcohol **97** and then mesylate **98**. Thus, these sequences provide access to useful intermediates carrying this Janus face ring system.

The methyl group was also explored as an alternative blocking group as shown in Figure 22. To achieve this benzonitrile **99** was subject to a Birch reduction, quenching with methyl iodide.[54] This generated cyclohexadiene **100**, which was then converted to the diepoxide stereoisomers **101a-c**.

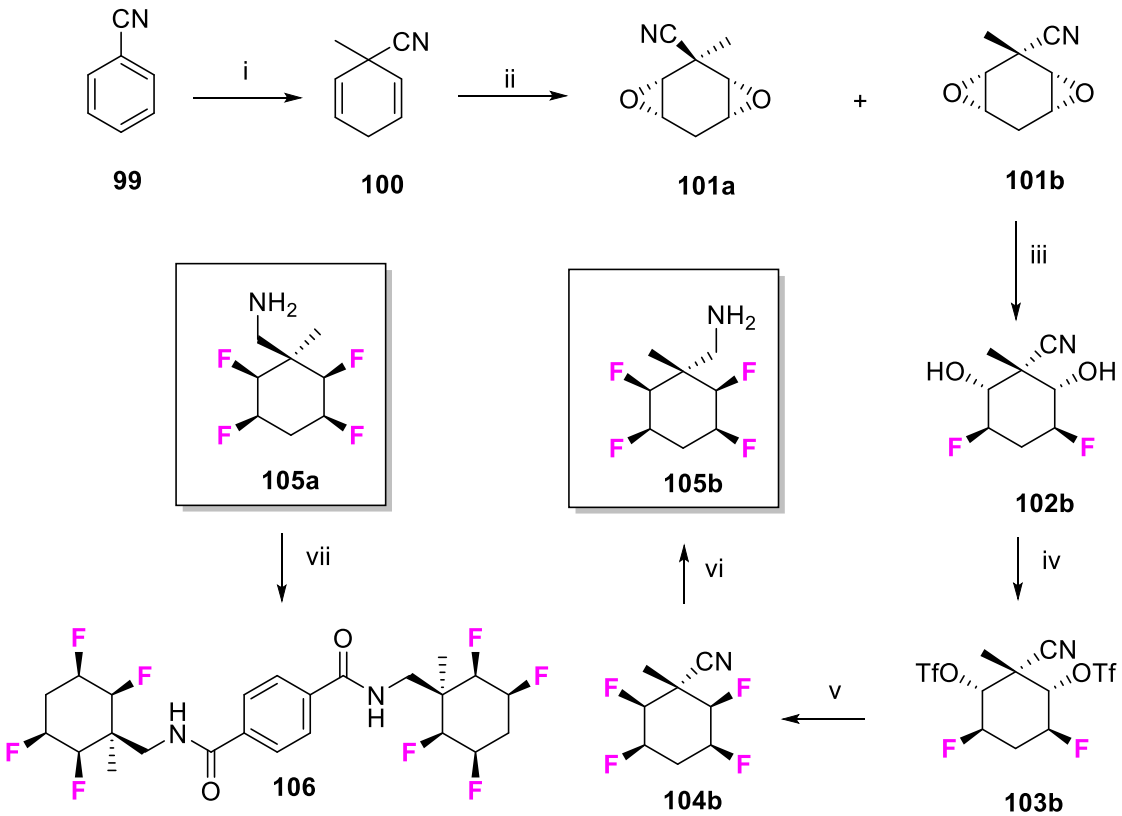

Figure 22: Amine building blocks: i. Li, NH_3, *t*BuOH, MeI, 3h, -78°C, 18 h, rt, 31%; ii. *m*CPBA, DCM, 48h, 35 °C, 53%; iii. $Et_3N.3HF$, 18h, 140°C; iv. Tf_2O, pyridine, 1h, 0 °C, 3h, rt, 30%; v. $Et_3N.3HF$, 4 d, 120 °C, 30%; vi. $NaBH_4$/ $NiCl_2.6H_2O$, MeOH, 1h, 0°C, 18h, rt, 50%; vii. Terephthaloyl chloride (3 eq), $Et_3.N$, DMAP (2 mol %), DCM, 18 h, rt, 48%.[54]

10.1002/chem.202000178

Intermediate **104b** is now stable to dehydrofluorination due to the methyl group, and the nitrile is now amenable to various functional group transformations including its reduction to an amino-methylene. Figure 22 highlights routes to both diastereoisomers of amines **105** with the amino-methylene group either on the fluorine face **105a** or the hydrogen face, **105b** of the Janus ring. These amines were progressed as individual stereoisomers to *bis*-amides such as **106**.

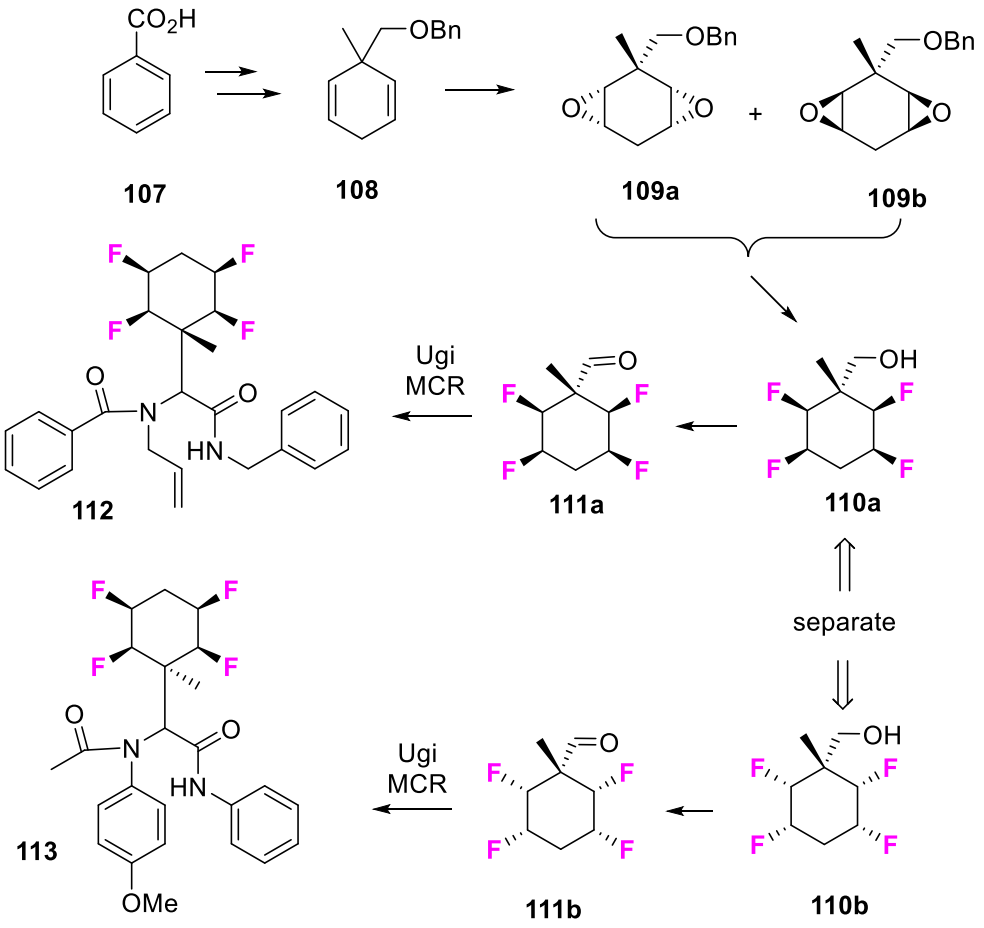

Figure 23: Methyl blocked, alcohol and aldehyde tetrafluorocyclohexane building blocks used for multicomponent reactions.[55]

In a variant of the previous protocol, benzoic acid **107** was also subject to a Birch reduction, followed by a methyliodide quench as illustrated in Figure 23.[55] After reduction and benzyl protection, diepoxidation of benzyl ether **108** generated a mixture of *syn* and *anti* diepoxide diastereoisomers (plus a minor *anti* isomer - not shown) **109a** and **109b**. These were progressed separately to the all-*syn* tetrafluorocyclohexane hydroxymethyl alcohols **110a** and **110b** as

10.1002/chem.202000178

described in detail elsewhere.[55] Oxidation of these alcohols to their corresponding aldehydes **111a** and **111b** generated useful building blocks which were used as the aldehyde in Ugi and Passerini multicomponent reactions to generate compounds exemplified by **112** and **113**. Thus these building blocks allow access to diverse molecular architectures carrying these unique ring motifs.

All-*syn* 1,2,3,4,-Tetrafluorocyclopentane

As part of this programme a route to all-*syn* tetrafluorocyclopentane **116** was developed.[33] This compound was prepared from freshly cracked cyclopentadiene **114**, which was progressed to the known *syn* diepoxide **115**. Progressive deoxyfluorinations of **115** were readily achieved and **116** could be prepared in a straightforward manner. The polar nature of cyclopentane **116** was immediately obvious in that it was a crystalline solid (mp 39 ^{o}C), and the Janus face aspect of the molecule was again apparent comparing ^{1}H-NMR spectra in $CDCl_3$ and toluene as solvents. Anisotropically induced upfield chemical shifts in toluene, were particularly large for all of the hydrogen atoms on the electropositive face of the ring indicative of an association between the alicyclic ring and the aromatic ring of the solvent. Consistent with this, hydrogen (H5b), the only hydrogen on the electronegative fluorine face of the ring, had the smallest change in chemical shift. The molecular packing in the X-ray derived crystal structure of **116** is clearly ordered electrostatically, where the rings are stacked one on top of another and with the fluorine faces contacting the hydrogen faces of adjacent molecules, as illustrated in Figure 24c.

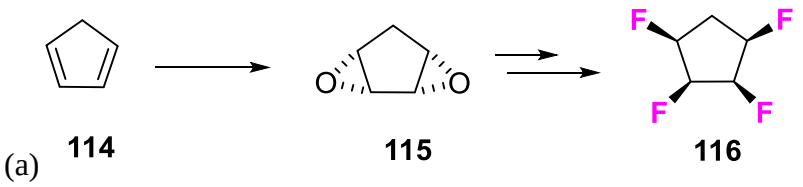

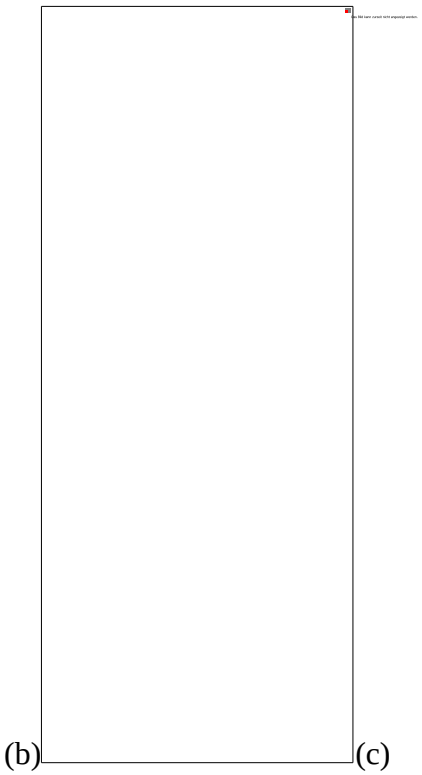

(b)

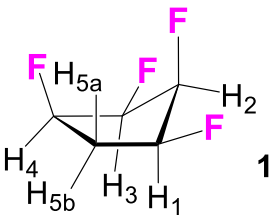

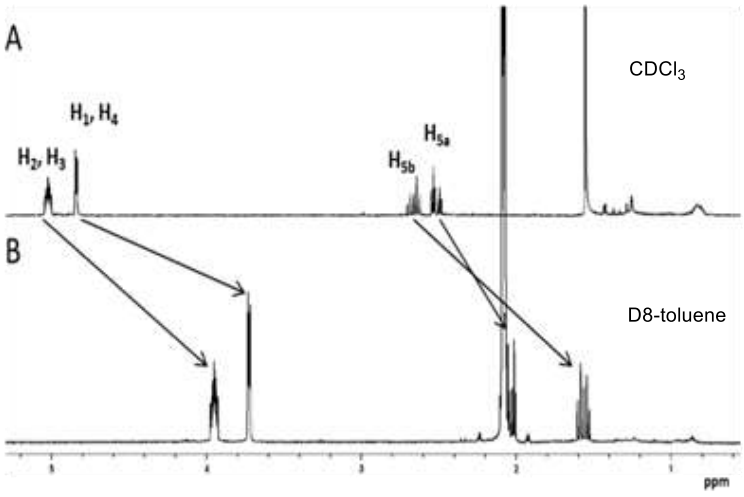

(c)

Figure 24: (a) Synthesis approach to **116**. (b) X-Ray structure of **116** showing molecular packing and (c) ^{1}H-NMR of **116** is A $CDCl_3$ and B [$^{2}H_8$]-toluene illustrating large anisotropically induced chemical shifts in toluene for the hydrogen face protons .[33]

All *syn* 1,2,3-trifluorocyclopropane.

In contrast to cyclohexane and cyclopentane, the cyclopropane ring is conformationally rigid and thus there are entropic advantages to using such a motif in the development of pharmaceutical candidates. Selectively fluorinated cyclopropanes have received some attention in this respect but are almost entirely confined to monofluorination.[56] There are no examples of *syn* or *anti* 1,2,3-trifluoro-cyclopropanes recorded in bioactives discovery chemistry. Clearly placing three fluorines on one face of the cyclopropane ring as found in the *syn* isomer, should

10.1002/chem.202000178

induce a significant Janus face polarity and a unique physiochemical property relative to cyclopropane itself. Therefore it became a focus to prepare such a cyclopropane. The parent compound 1,2,3-trifluorocyclopropane **118** had been prepared and isolated at an analytical level, by Gillies in the 1970s.[57] The two isomers (*syn* **118a** and *anti* **118b**) emerged as volatiles from the ozonolysis of *cis*-1,2-difluoroethene **117** as shown in Figure 25, presumably by *in situ* generation of monofluorocarbene and then addition of the carbene to the excess olefin. Isolation by prep GC generated sufficient material for characterisation by microwave and vibrational spectroscopy, however this material was never made on a preparative scale.

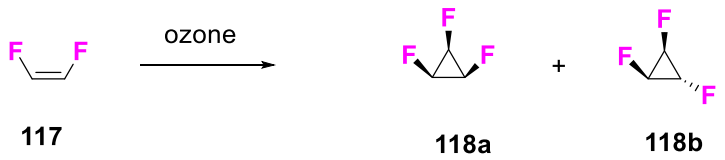

Figure 25: *Syn* and *anti* isomers of 1,2,3-trifluorocyclopropane **118** were identified by Gillies as volatiles from ozonolysis of *cis*-1,2-DFE **117**.[57]

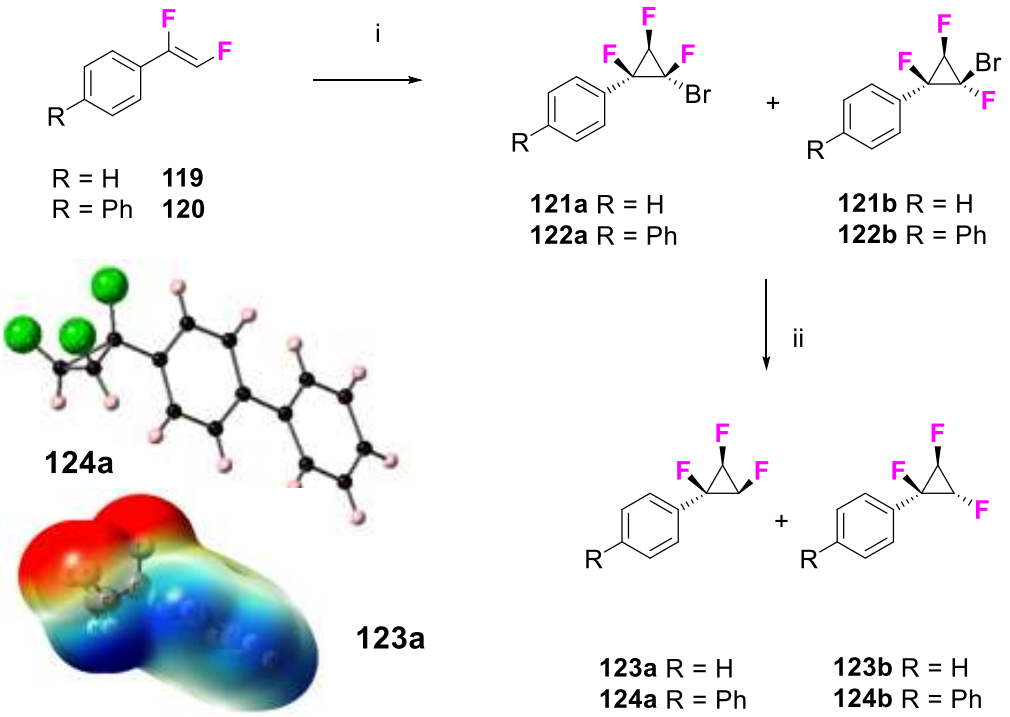

Figure 26: i. $CHFBr_2$, TEBAB, $NaOH{\cdot}H_2O$, DCM, 0 °C-RT, 21-26%; ii. Bu_3SnH, AIBN, RT, 37-42%. Synthesis of *syn* and *anti* isomers of 1,2,3-trifluorocyclopropanes **119** & **120** with an X-ray structure of the all-syn isomer **124a** and an electrostatic surface potential map of all-*syn* **123a**.[34]

Our approach[34] envisaged a fluorocarbene addition to a *Z*-α,β-difluoro styrene such that an aryl cyclopropane derivative could be prepared and which would be amenable to further elaboration to useful building blocks. Accordingly, we focussed on carbene additions to α,β-difluoro difluorostyrenes *Z*-**119** and *Z*-**120** as illustrated in Figure 26. The olefin is deactivated due to the presence of the two fluorines and all attempts at direct monofluorocarbene (HFC:) addition failed. The more electrophilic halofluorocarbenes (HXC:) were more successful, but this left the challenge of navigating a reductive removal of the non-fluoro halogen, without concomitant cyclopropane ring opening. Although addition of chlorofluorocarbene (HClC:) to *Z*-**119** and *Z*-**120** generated the resultant cyclopropane isomers, harsh conditions were required to reductively remove the chlorine, and this led to an intractable product mixture. Both bromofluoro and iodofluoro carbenes also generated the corresponding cyclopropane isomers, however in our hands reductive dehalogenation of the bromocyclopropane products **121** and **122**, with tributyltin hydride, offered the only practical access to 1,2,3-trifluorocyclopropanes **123** and **124**. In this manner all-*syn* 1,2,3,-trifluorocyclopropanes **123a** and **124a** were prepared and characterised, as were the *anti* isomers **123b** and **124b.** The X-ray structure of **124a** confirmed that the three fluorines orient to one face of the cyclopropane ring. An electrostatic surface potential map for the all-*syn* isomer **123a** in Figure 26 illustrates clearly the different polarity on each face of the ring (electronegative fluorine face in red and the electropositive hydrogen face in blue). This ring comes into the class of Janus face cycloalkyls. In the next section the Log P's of several phenyl derivatives of partially fluorinated cycloalkanes are compared against other substituents and it is emerges that the *syn*-1,2,3-trifluorocyclopropane **123a** is the most polar of those studied.

Log Ps and polarity.

There has been a long history regarding the introduction of fluorine containing substituents into pharmaceuticals and agrochemicals products, the most common being aryl-F, aryl CF_3 and aryl O-CF_3. As previously discussed aryl fluorinated substituents raise the LogP of a drug candidate relative to their hydrocarbon counterparts aryl-H, aryl-CH_3 and ary-OCH_3. This is illustrated in Figure 27 for benzene, toluene and anisole where the changes in Log P gets progressively larger with -F, to -CF_3 and then to OCF_3 substitutions. The discussion in this review has focussed on partially fluorinated alicyclic rings. It can be seen in Figure 27 that all-*syn* 1,2,4,5-

10.1002/chem.202000178

tetrafluorocyclohexane **71** and all-*syn* 1,2,3-trifluorocyclopropane **123a** have the lowest Log Ps in the series and are the most polar. [34,58]

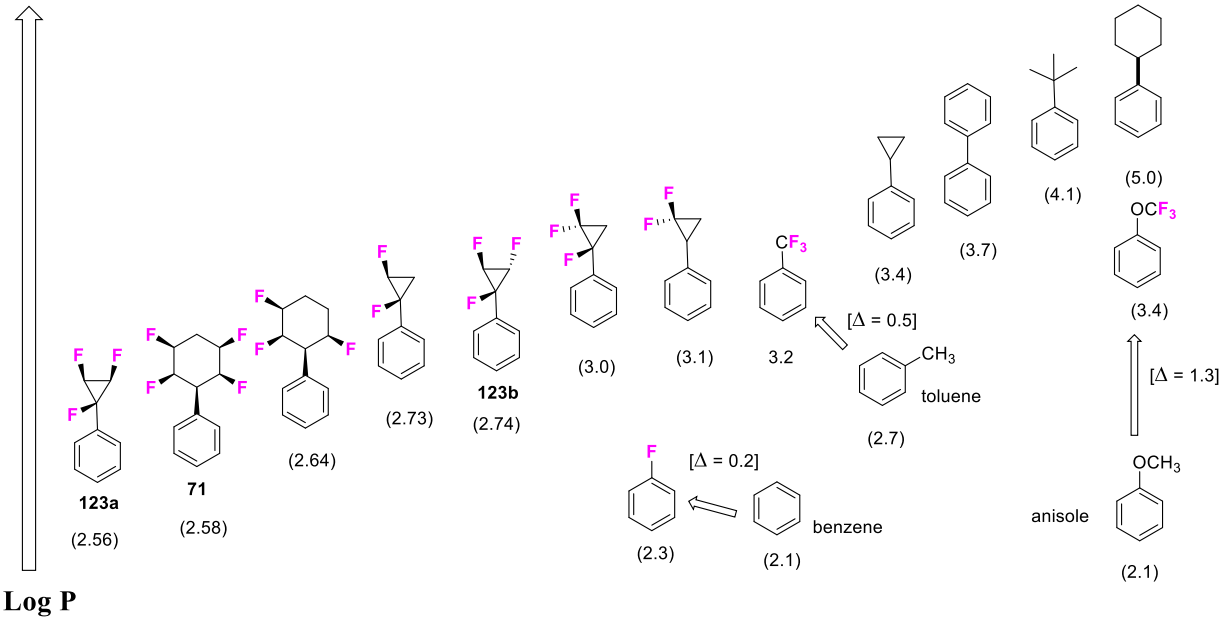

Figure 27: Comparison of the changes in Log P of selected alkyl and fluoroalkyl substituents. Experimental Log P (values) are given in brackets and structures are represented with increasing Log P (not to scale).[34,58]

A comparison of trifluorocyclopropanes **123a** and **123b** illustrates that the all-*syn* isomer **123a** is the more polar consistent with the three fluorine on one face of the ring. Also from the array of partially fluorinated cyclopropane rings represented here, all are more polar than phenylcyclopropane itself.

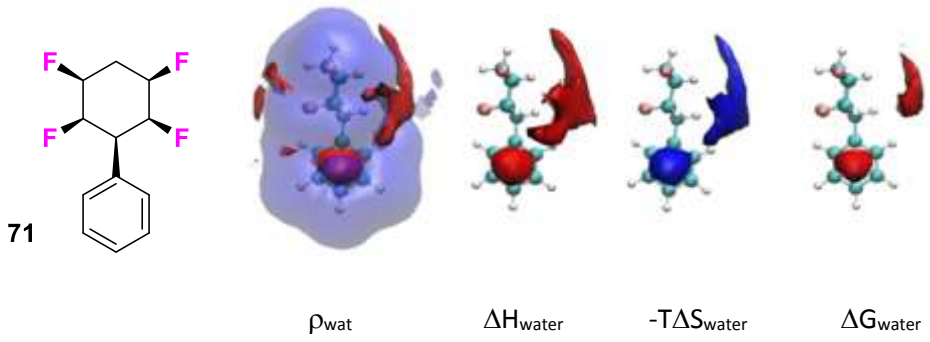

Figure 28: Molecular dynamics illustrates a thermodynamic preference for water molecules to associate with the hydrogen face of the cyclohexane ring of **71**. The maps illustrate water density (ρ_{wat}), enthalpic (ΔH) stabilisation, entropic ($-T\Delta S$) destabilisation and overall free energy (ΔG) stabilisation of organised water relative to the bulk solvent.[58]

It is notable from Figure 27, that the placement of the four fluorine atoms on the cyclohexane ring reduces the Log P of **71** (Log P = 2.6) by almost 2.5 Log units relative to phenylcyclohexane (Log P = 5.0), and that **71** has a similar Log P to trifluorocyclopropane **123a** (Log P = 2.56), despite having three more carbon and four more hydrogen atoms. This is the most dramatic example, within this class of molecules, of the effect that selective fluorination has on increasing polarity. A molecular dynamics study[58] exploring the interaction of tetrafluorocyclohexane **71** with water, revealed that water interacts with the hydrogen face, rather than the fluorine face of the cyclohexane ring. This is illustrated in the various thermodynamic maps in Figure 28. Enthalpic stabilisation dominated negative entropic effects, suggesting that electrostatic attraction (hydrogen bonding) between the polarised (geminal) hydrogens of the ring and the oxygen of water is the most significant interaction. This property of cyclohexane **71** illustrates the remarkable influence of selective fluorination on aliphatic polarity and increases the relevance for exploring the motif and its derivatives in bioactive discovery programmes.

Concluding remarks

The review has summarised the development of multivicinal fluoromethylenes as a new class of organofluorine compounds. An initial focus on alkane chains of this class has developed to alicyclic rings. Notably for the Janus face cyclohexane and cyclopropane systems significant polarities are achieved, and they have the capacity to coordinate cations and anions and hydrogen bond to water. In the next phase it will be exciting to explore how these rings interact with proteins and to assess their potential as motifs for drug discovery. This will only be realised if efficient routes become available for the preparation of building blocks, however there is no doubt that the attention of the methodology community is beginning to impact. As discussed, important developments are being made here which should facilitate easier and better access to higher order multivicinal fluoroalkanes, offering exciting prospects for the future in both bioactives and materials programmes.

Acknowledgements

I am grateful to my co-workers who contributed to this programme over a good number of years. The preparation of many of the multivicinal fluorine targets was extremely hard won

and demanded considerable technical skill, insight and perseverance. The effort was compensated for by the joy of making these compounds and exploring their properties.

References

1. (a) N. A. Meanwell, *J. Med. Chem.,* **2018**, *61*, 5822–5880; (b) E. P. Gillis, K. J. Eastman, M. D. Hill, D. J. Donnelly, N. A. Meanwell, *J. Med. Chem.*, **2015**, *58*, 8315 – 8359; (c) J. Wang, M. Sánchez-Roselló, J. L. Aceña, C. del Pozo, A.E. Sorochinsky, S. Fustero, V. A. Soloshonok, H. Liu, *Chem. Rev.*, **2014**, *114*, 2432-2506 ; (d) W. K. Hagmann, *J. Med. Chem.*, **2008**, *51*, 4359–4369.
2. (a) Y. Zafrani, G. Sod-Moriah, D. Yeffet, A. Berliner, D. Amir, D. Marciano, S. Elias, S. Katalan, N. Ashkenazi, M. Madmon, E. Gershonov, S. Saphier, *J. Med. Chem*., **2019**, *62*, 5628 – 5637; (b) N. Erdeljac, G. Kehr, M. Ahlqvist, L. Knerr, R. Gilmour, *Chem. Commun.*, **2018**, *54*, 12002 – 12005; (c) B. Linclau, Z. Wang, G. Compain, V. Paumelle, C. Q. Fontenelle, N. Wells, A. Weymouth-Wilson, *Angew. Chem. Int. Ed.*, **2016**, *55*, 674-678;
3. (a) L. Hunter, *Beilstein J. Org. Chem.,* **2010,** *6*, 38; (b) D. O'Hagan. *Chem. Soc. Rev.*, **2008**, *37*, 308 – 319.
4. B. E. Smart, *J. Fluorine Chem*., **2001**, *109*, 3-11.
5. M. G. Campbell, T. Ritter, *Chem. Rev*., **2015**, *115*, 612-633.
6. C-C. Tseng, G. Baillie, G. Donvito, M. A. Mustafa, S. E. Juola, C. Zanato, C. Massarenti, S. Dall'Angelo, W. T. A. Harrison, A. H. Lichtman, R. A. Ross, M. Zanda, I. R. Greig; J. Med. Chem., **2019**, *62*, 5049-506.
7. (a) G. Landelle, A. Panossian, F. R. Leroux, *Curr Top Med Chem.,* **2014**, *14*, 941-951; (b) F. R Leroux, B. Manteau, J-P Vors, S. Pazenok, *Beilstein J. Org. Chem.,* **2008**, *4*, 13.
8. Q. A. Huchet, N. Trapp, B. Kuhn, B. Wagner, H. Fischer, N. A. Kratochwil, E. M. Carreira, K. Müller, *J. Fluorine. Chem*., **2017**, *198*, 34 – 46; (b) R. Vorberg, N. Trapp, D. Zimmerli, B. Wagner, H. Fischer, N. A. Kratochwil, M. Kansy, E. M. Carreira, K. M Müller, *ChemMedChem*, **2016**, *11*, 2216 – 2239; (c) Q. A. Huchet, B. Kuhn, B. Wagner, N. A. Kratochwil, H. Fischer, M. Kansey, D. Zimmerli, E. M. Carreira, K. Müller, *J. Med. Chem*., **2015**, *58*, 9041 – 9060.
9. This information is in the public domain but was sourced (January 2020) here from the federal Drug Administration data base; *Drugs@FDA: FDA-Approved Drugs.*
10. (a) A. Rodil, A. M. Z. Slawin, N. Al-Maharik, R. Tomita, D. O'Hagan, *Beilstein J. Org. Chem.,* **2019**, *15*, 1441-1447; (b) R. Tomita, N. Al-Maharik, A. Rodil, M. Bühl, D. O'Hagan, *Org. Bio.Chem.,* **2018**, *16*, 1113–1117; (c) D. Bello, D. O'Hagan, *Beilstein J. Org. Chem.,* **2015**, *11*, 1902-1909.

11. L. Xing, D. C. Blakemore, A. Narayanan, R. Unwalla, F. Lovering, R. A. Denny, H. Zhou, M. E. Bunnage, *ChemMedChem.*, **2015**, *10*, 715– 726.
12. B. Jeffries, Z. Wang, J. Graton, S. D. Holland, T. Brind, R. D. R. Greenwood, J. Y. Le Questel, J. S. Scott, E. Chiarparin, B. Linclau, *J. Med. Chem.*, **2018**, *61*, 10602-10618.
13. D. O'Hagan, *J. Org. Chem.*, **2012**, *77*, 3689–3699.
14. (a) S. Bresciani, T. Lebl, A. M. Z. Slawin, D. O'Hagan, *Chem. Commun.*, **2010**, *46*, 5434 – 5436; (b) V. A. Brunet, D. O'Hagan, A. M. Z. Slawin, *Beilstein J. Org. Chem.*, **2009**, *5*, 61; (b) M. Nicoletti, M. Bremer, P. Kirsch, D. O'Hagan, *Chem. Commun.*, **2007**, 5075 – 5077; (c) M. Nicoletti, A. M. Z. Slawin, D. O'Hagan, *J. Am. Chem. Soc.*, **2005**, *127*, 482 - 483.
15. (a) L. Hunter, D. O'Hagan, *Org. Biol. Chem.*, **2008**, *6*, 2843 – 2848; (b) L. Hunter, P. Kirsch. J. T. G. Hamilton, D. O'Hagan, *Org. Biol. Chem.*, **2008**, *6*, 3105- 3108; (c) L. Hunter, D. O'Hagan, *Angew.Chemie.,Int. Ed.*, **2007**, *46*, 7887 – 7890; (d) L. Hunter, D. O'Hagan, A. M. Z. Slawin, *J. Am. Chem. Soc.*, **2006**, *128*, 16422 - 16423.
16. D. Farran, A. M. Z. Slawin, P. Kirsch, D. O'Hagan, *J. Org. Chem.*, **2009**, *74*, 7168 – 7171.
17. L. Hunter, P. Kirsch, A. M. Z. Slawin, D. O'Hagan, *Angew. Chem. Int. Ed.*, **2009**, *48*, 5457 - 5460.
18. (a) A. J. Durie, A. M. Z. Slawin, T. Lebl, P. Kirsch, D. O'Hagan, *Chem Commun.*, **2012**, *48*, 9643-9645. (b) A. J. Durie, A. M. Z. Slawin, T. Lebl, P. Kirsch, D. O'Hagan, *Chem Commun.*, **2011**, *47*, 8265 - 8267.
19. A. J. Durie, A. M. Z. Slawin, T. Lebl, D. O'Hagan, *Angew. Chemie. Int. Ed.*, **2012**, *51*, 10086 - 10088.
20. N. S. Keddie, A. M. Z. Slawin, T. Lebl, D. Philp, D. O'Hagan, *Nature Chem.*, **2015**, *7*, 483-488.
21. N. Santschi, R. Gilmour, *Nature Chem.*, **2015**, *7*, 467 – 468.
22. (a) F. A. Martins, M. P. Freitas, *Eur. J. Org. Chem.*, 2019, 6401 – 6406; (b) C. Thiehoff, Y. P. Rey, R. Gilmour, *Isr. J. Chem.*, **2017**, *57*, 92-100; (c) S. Wolfe, *Acc. Chem. Res.*, **1972**, 5, 102 – 111.
23. S. J. Fox, S. Gourdain, A. Coulthurst, C. Fox, I. Kuprov, J. W. Essex, C. K. Skylaris, B. Linclau, *Chem. Eur. J.*, **2015**, *21*, 1682-1691.
24. S. Rozen, M. Brand, *J. Org. Chem.*, **1986**, *51*, 3607-3611.
25. T. Hamatani, S. Matsubara, H. Matsuda, M. Schlosser, *Tetrahedron*, **1988**, *44*, 2875-2881.
26. M. Schűler, A. M. Z. Slawin, D. O'Hagan, *Chem Commun.*, **2005**, 4324 – 4326.
27. (a) X. G. Hu, D. S. Thomas, R. Griffith, L. Hunter, *Angew. Chemie. Int. Ed.*, **2014**, *53*, 6176 – 6179; (b) L. Hunter, S. Butler, S. B. Ludbrook, *Org. Biomol. Sci.*, **2012**, *10*, 8911-8918; (c) L. Hunter, K. A. Jolliffe, M. J.T. Jordan, P. Jensen, R. B. Macquart, *Chem. Eur. J.*, **2011**, *17*, 2340 – 2343.
28. C. Au, C. Gonzalez, Y. C. Leung, F. Mansour, J. Trinh, Z. Y. Wang, X. G. Hu, R. Griffith, E. Pasquier, L. Hunter, *Org. Biol. Chem.*, **2019**, *17*, 664- 674.

29. (a) C. R. S. Briggs, D. O'Hagan, J. A. K. Howard, D. S. Yufit, *J. Fluorine Chem.*, **2003**, *119*, 9-13; (b) E. Cosimi, N. Trapp, M-O. Ebert, H. Wennemers, *Chem. Commun.*, **2019**, *55*, 2253-2256.
30. I. Yamamoto, M. J. T. Jordan, N. Gavande, M. R. Doddareddy, M. Chebib, L. Hunter, *Chem. Commun.*, **2012**, *48*, 829-831.
31. S. Hara, J. Nakahigashi, K. Ishi-i, M. Sawaguchi, H. Sakai, T. Fukuhara, N. Yoneda, *Synlett*, **1998**, *1998*, 495-496.
32. (a) S. M. Banik, J. W. Medeley, E. N. Jacobsen, *J. Am. Chem. Soc.*, **2016**, *138*, 5000-5003. (b) K. M. Haj, S. M. Banik, E. N. Jacobsen, *Org. Lett.*, **2019**, *21*, 4919 – 4923;
33. (a) I. G. Molnár, R. Gilmour, *J. Am. Chem. Soc.*, **2016**, *138*, 5004-5007; (b) F. Scheidt, M. Schäfer, J. C. Sarie, C. D. Daniliuc, J. J. Molloy, R. Gilmour, *Angew. Chem. Int. Ed*., **2018**, *57*, 16431-16435.
34. S. Doobary, A. T. Sedikides, H. P. Caldora, D. L. Poole, A. J. J. Lennox, *Angew. Chemie. Int. Ed.*, **2020**, *59*, 1155 – 1160.
35. N. Al-Maharik, D. B. Cordes, A. M. Z. Slawin, D. O'Hagan, *Org. Biomol. Sci.*, **2020,** *18*, 878-887.
36. P. Bentler, N. Erdeljac, K. Bussmann, M. Ahlqvist, L. Knerr, K. Bergander, C. Daniliuc, R. Gilmour, *Org. Lett.*, **2019**, *21*, 7741-7745.
37. Z. Fang, N. Al-Maharik, A. M. Z. Slawin, M. Bühl, D. O'Hagan, *Chem Commun.*, **2016**, *52*, 5116 – 5119.
38. Z. Fang, D. B. Cordes, A. M. Z. Slawin, D. O'Hagan, *Chem. Commun.*, **2019**, *55*, 10539 – 10542.
39. See, E. L. Eliel, S. H. Wilen, '*Stereochemistry of Organic Compounds'* John Wiley & Sons Inc., **1994**, New York.
40. (a) E. Juaristi, R. Notario, *J. Org. Chem.*, **2016**, *81*,1192-1197; (b) Q. Luo, K. R. Randall, H. F. Schaefer, *RSC Adv*., **2013**, *3*, 6572-6585; (c) Z. Zdravkovski, *Bull. Chem. Technol. Maced.*, **2004**, *23*, 131– 137.
41. (a) M. P. Wiesenfeldt, Z. Nairoukh, W. Li, F. Glorius, *Science*, **2017**, *357*, 908-912; (b) M. P. Wiesenfeldt, T. Knecht, C. Schlepphorst, F. Glorius, *Angew. Chemie. Int. Ed.*, **2018**, *57*, 8297--8300.
42. P. L. Coe, R. G. Plevey, J. C. Tatlow, *J. Chem. Soc. C.*, **1969**, 1060 - 1063.
43. Z. Zweig, R. G. Fischer, J. E. Lancaster, *J. Org. Chem.*, **1980**, *45*, 3597 – 3603.
44. L. Ling, Y. He, X. Zhang, M. Luo, X. Zeng, *Angew. Chem. Int. Ed.*, **2019**, *58*, 6554–6558; (b) Y. Wei, B. Rao, X. Cong, X. Zeng, *J. Am. Chem. Soc.*, **2015**, *137*, 9250–9253.
45. Z. Nairoukh, M. Wollenburg, C. Schlepphorst, K. Bergander, F. Glorius, *Nature Chem*., **2019**, *11*, 264-270.

46. (a) B. E. Ziegler, M. Lecours, R. A. Marta, J. Featherstone, E. Fillion, W. S. Hopkins, V. Steinmetz, N. S. Keddie, D. O'Hagan, T. B. McMahon, *J. Am. Chem. Soc.*, **2016**, *138*, 7460 - 7463; (b) M. J. Lecours, R. A. Marta, V. Steinmetz, N. Keddie, E. Fillion, D. O'Hagan, T. B. McMahon, W. S. Hopkins, *J. Phys. Chem. Letts.*, **2017**, *8*, 109 - 113.
47. O. Shyshov, K. A. Siewerth, M. von Delius, Max, *Chem. Commun.*, **2018**, *54*, 4353-4355.
48. (a) Sun, Wei-Ming; Ni, Bi-Lian; Wu, Di; Lan, Jian-Ming; Li, Chun-Yan; Li, Ying; Li, Zhi-Ru; *Organometallics*, **2017**, *36*, 3352-3359; (b) F. Y. Naumkin, *J. Phys. Chem. A.*, **2017**, *121*, 4545-4551.
49. (a) J. J. Wang, Y. D. Song, Q. T. Wang, *Theor. Chem. Acc.*, **2020**, *139*, 4; (b) Y. F. Wang, J. Li, J. G. Huang, T. Qin, Y. M. Liu, F. Zhong, W. Zhang, Z. R. Li, *J. Phys. Chem. C.*, **2019**, *123*, 23610-23619; (c) J. H. Hou, L. S Zhu, D. Y. Jiang, J. M. Qin, Q. Duan, *Chem. Phys. Lett.*, **2018**, *711*, 55-59.
50. (a) A. J. Durie, T. Fujiwara, N. Al-Maharik, A. M. Z. Slawin, D. O'Hagan, *J. Org Chem.*, **2014**, *79*, 8228-8233; (b)A. J. Durie, T. Fujiwara, R. Cormanich, M. Bühl, A. M. Z. Slawin, D. O'Hagan, *Chem.. Eur. J.*, **2014**, *20*, 6259-6263.
51. M. S. Ayoup, D. B. Cordes, A. M. Z. Slawin, D. O'Hagan, *Beilstein J. Org. Chem.*, **2015**, *11*, 2671–2676.
52. M. S. Ayoup, D. B. Cordes, A. M. Z. Slawin, D. O'Hagan, *Org. Biol. Chem.*, **2015**, *13*, 5621 – 5624.
53. T. Bykova, N. Al-Maharik, A. M. Z. Slawin, M. Bühl, T. Lebl, D.O' Hagan, *Chem. Eur. J.*, **2018**, *24*, 13290 - 13296.
54. T. Bykova, N. Al-Maharik, A. M. Z. Slawin, D. O'Hagan, *Beilstein J. Org. Chem.*, **2017**, *13*, 728-733.
55. T. Bykova, N. Al-Maharik, A. M. Z. Slawin, D. O'Hagan, *Org. Biol. Chem.*, **2016**, *14*, 1117 - 1123.
56. (a) K. Bartels, B. Schinor, G. Haufe, *J. Fluorine Chem.*, **2017**, *203*, 200-205; (b) A. Pons, T. Poisson, X. Pannecoucke, A. B. Charrette, P. Jubault, *Synthesis*, **2016**, *48*, 4060-4071; (c) B. Schinor, B. Wibbeling, G. Haufe, *J. Fluorine Chem.*, **2013**, *155*, 102-109; (d) K. Sakagami, A. Yasuhara, S. Chaki, R. Yoshikawa, Y. Kawakita, A. Saito, T. Taguchi, A. Nakazato, *Bioorg. Med. Chem.*, **2008**, *16*, 4359–4366; (e) S. Hruschka, R. Fröhlich, P. Kirsch, G. Haufe, *Eur. J. Org. Chem.*, **2007**, 141-148; (f) S. Yoshida, T. C. Rosen, O. G. J. Meyer, M. J. Sloan, S. Ye, G. Haufe, K. L. Kirk, *Biorg. Med. Chem.*, **2004**, *12*, 2645-2652.
57. (a) C. W. Gillies, *J. Am. Chem. Soc.*, **1975**, *97*, 1276 – 1278; (b) C. W. Gillies, *J. Mol. Spec.*, **1976**, *59*, 482-492; (c) R. N. Beauchamp, J. W. Agopovich, C. W. Gillies, *J. Am Chem. Soc.*, **1986**, *108*, 2556 – 2560; (d) J. W. Agopovich, C. W. Gillies, *J. Am Chem. Soc.*, **1983**, *105*, 5047 – 5053.
58. A. Rodil, S. Bosisio, M. S. Ayoup, L. Quinn, D. B. Cordes, A. M. Z. Slawin, C. D. Murphy, J. Michel, D. O'Hagan, *Chem. Sci.*, **2018**, *9*, 3023 – 3028.

10.1002/chem.202000178